

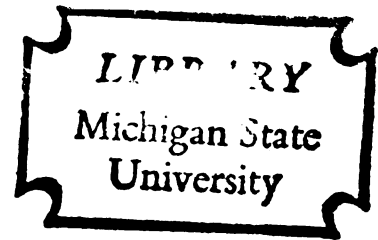
SURFACE AND ELECTROCHEMICAL
PROPERTIES OF PLANT CUTICLES

Thesis for the Degree of Ph. D.
MICHIGAN STATE UNIVERSITY
JÖRG SCHÖNHERR
1972



3 1293 10445 3356

IMÉDIT



This is to certify that the

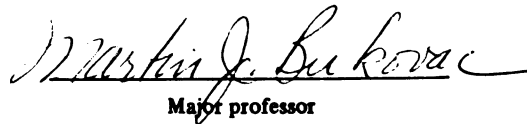
thesis entitled

Surface and Electrochemical
Properties of Plant Cuticles
presented by

Jörg Schönherr

has been accepted towards fulfillment
of the requirements for

Ph D degree in Horticulture


Major professor

Date June 9, 1972

0-7639



029

AUG 31 2012



ABSTRACT

SURFACE AND ELECTROCHEMICAL PROPERTIES OF PLANT CUTICLES

- I. *PENETRATION OF STOMATA BY LIQUIDS:
DEPENDENCE ON SURFACE TENSION,
WETTABILITY AND STOMATAL MORPHOLOGY.*
- II. *ION EXCHANGE PROPERTIES OF ISOLATED
TOMATO FRUIT CUTICULAR MEMBRANES:
EXCHANGE CAPACITY, NATURE OF FIXED
CHARGES AND CATION SELECTIVITY.*

By

Jörg Schönherr

Section 1

Wettability of the leaf surface, surface tension of the liquid and stomatal morphology control penetration of stomata by liquids. The critical surface tension of the lower leaf surface of *Zebrina purpusii*, Brückn., was estimated to be 25 to 30 dyne cm⁻¹. Liquids having a surface tension less than 30 dyne cm⁻¹ gave zero contact angle on the leaf surface and infiltrated stomata spontaneously while liquids having a surface tension greater than 30 dyne cm⁻¹ did not wet the leaf surface and failed to infiltrate stomata. Considering stomata

as conical capillaries we were able to show that with liquids giving a finite contact angle, infiltration depended solely on the relationship between the magnitude of the contact angle and the wall angle of the aperture. Generally, spontaneous infiltration of stomata will take place when the contact angle is smaller than the wall angle of the aperture wall. The degree of stomatal opening (4, 6, 8 or 10 μm) was of little importance. Cuticular ledges present at the entrance to the outer vestibule and substomatal chamber resulted in very small if not zero wall angles, and thus played a major role in excluding water from the intercellular space of leaves. We show why the degree of stomatal opening cannot be assessed by observing spontaneous infiltration of stomata by organic liquids of low surface tension.

Section II

Isolated tomato fruit cuticular membranes free of extractable materials were titrated potentiometrically using various bases. Three distinctly different dissociable groups were observed in the pH ranges 3 to 6 (0.2 meq g^{-1}), 6 to 9 (0.3 meq g^{-1}) and 9 to 12 (0.55 meq g^{-1}). The first group was tentatively assigned to $-\text{COOH}$ groups of pectic materials and protein embedded in the membrane, the second to non-esterified $-\text{COOH}$ groups of the cutin polymer and the third to phenolic $-\text{OH}$ groups

such as non-extractable flavonoids present in the membranes as well as to a small amount of $-\text{NH}_3^+$ groups of proteins. The cuticular membranes exhibited a behavior typical of highly cross-linked, high-capacity ion exchange resins of the weak-acid type. Ion exchange capacity increased with increasing pH and neutral salt concentration. At constant pH and salt concentration, the exchange capacity increased with increasing counterion valence and decreasing crystal radius, resulting in the following order: $[\text{tris (ethylenediamine) Co}]^{3+} \geq \text{Ca}^{2+} > \text{Ba}^{2+} > \text{Li}^+ > \text{Na}^+ > \text{Rb}^+ > \text{N}(\text{CH}_3)_4^+$. The cutin polymer exhibited a pronounced selectivity for Ca^{2+} over Na^+ which increased with increasing neutralization of fixed charges, while the large trivalent $[\text{Co}(\text{en})_3]^{3+}$ was preferred only at low equivalent ionic fractions of this counterion in the polymer. These results are discussed in relation to structure and function of cuticular membranes.

SURFACE AND ELECTROCHEMICAL PROPERTIES
OF PLANT CUTICLES

By

Jörg Schönherr

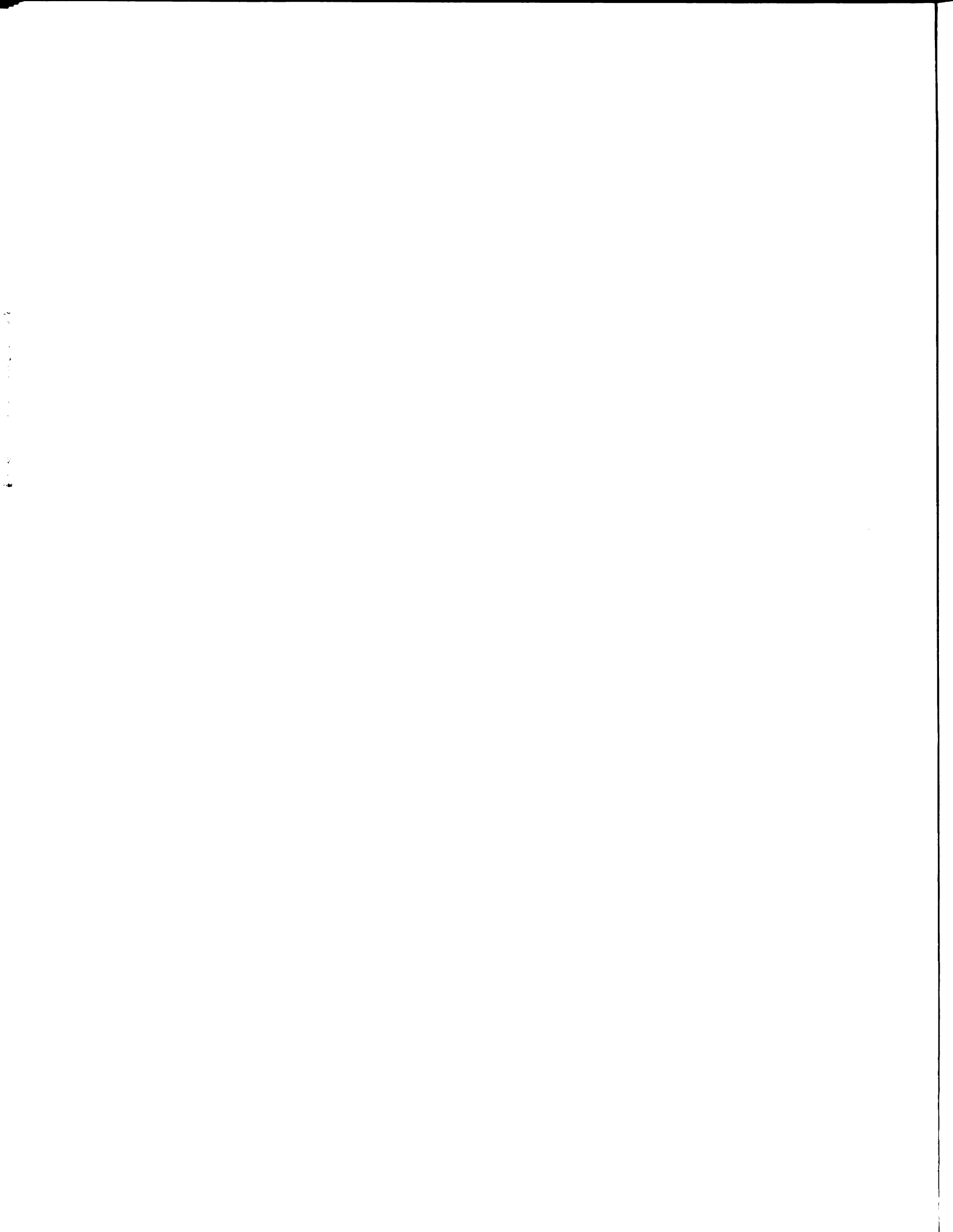
A THESIS

Submitted to
Michigan State University
in partial fulfillment of the requirements
for the degree of

DOCTOR OF PHILOSOPHY

Department of Horticulture

1972



ACKNOWLEDGMENTS

The author wishes to express his sincere appreciation to Dr. M. J. Bukovac for his counsel and guidance during the course of the experiments and in preparing the manuscripts. I am also most grateful to the members of my Guidance Committee: Drs. M. Mortland, K. Raschke, H. P. Rasmussen and M. Zabik. I also wish to thank Mrs. Elizabeth Shields for the ash analysis by atomic absorption spectroscopy.

This investigation was supported in part by Public Health Service Grant CC 00246 from the National Communicable Disease Center, Atlanta, Georgia, and Food and Drug Administration Grant FD 00223.

TABLE OF CONTENTS

	Page
ACKNOWLEDGMENTS	ii
LIST OF TABLES	iv
LIST OF FIGURES	v
GENERAL INTRODUCTION	viii
 <i>SECTION I: PENETRATION OF STOMATA BY LIQUIDS: DEPENDENCE ON SURFACE TENSION, WETTABILITY AND STOMATAL MORPHOLOGY</i>	
INTRODUCTION	2
THEORY	3
EXPERIMENTAL	9
RESULTS	13
DISCUSSION	22
LITERATURE CITED	30
 <i>SECTION II: ION EXCHANGE PROPERTIES OF ISOLATED TOMATO FRUIT CUTICULAR MEMBRANES: EXCHANGE CAPACITY, NATURE OF FIXED CHARGES AND CATION SELECTIVITY</i>	
INTRODUCTION	34
MATERIALS AND METHODS	35
RESULTS	39
DISCUSSION	61
REFERENCES	77

LIST OF TABLES

Table		Page
1.	Ash composition of TFCM	43
2.	Elemental composition of TFCM	48
3.	Exchange capacity of TFCM at pH 9.0 as function of nature and concentration of counterion . .	55
4.	Selectivity coefficients for the simultaneous exchange of Ca^{2+} and Na^{+} by TFCM	62
5.	Estimated contribution of proteins, pectic substances and flavonoids to the exchange capacity of TFCM.	68

LIST OF FIGURES

Figure		Page
<i>Section I</i>		
1.	Schematic drawing of conical capillary	5
2.	Schematic drawing of Amaryllis-type stoma	5
3.	Infiltration chamber	5
4.	Photomicrographs of leaf surface and stomata of <u>Z. purpusii</u>	14
5.	Effect of surfactant concentration on surface tension of aqueous solutions	17
6.	Contact angles formed on the lower surface of <u>Z. purpusii</u> by surfactant solutions of different surface tension (Zisman plot).	17
7.	Relationship between contact angle and pressure required to infiltrate stomata of <u>Z. purpusii</u>	20
8.	Effect of illumination period (800 ft.c.) of <u>Z. purpusii</u> leaves on pressure required to infiltrate stomata with a Tween 20 solution forming a contact angle of 63°.	20
9.	Comparison of observed and calculated infiltrating pressures	25
<i>Section II</i>		
1.	Titration of TFCM with Ca(OH)_2 in presence of 0.1 N CaCl_2 as affected by pretreatment of the TFCM	40
2.	Exchange capacity of TFCM as function of pH and CaCl_2 concentration	40
3.	Exchange capacity of TFCM at high pH values as determined by back titration and $^{45}\text{Ca}^{2+}$ - uptake.	46

Figure		Page
4.	Exchange capacity of TFCM after acid hydrolysis as a function of pH and CaCl_2 concentration	46
5.	Scanning electron micrographs of the morphological inner surface (cell-wall side) of TFCM before and after hydrolysis	50
6.	Henderson-Hasselbalch plot for the second dissociable group of TFCM	52
7.	Exchange capacities of cuticular membranes of pepper fruit, tomato fruit cv. "Traveller" and <u>Brassaia</u> leaf as a function of pH at 0.1 N CaCl_2 concentration	52
8.	Exchange capacity of TFCM as a function of pH and nature of the counterion	56
9.	Exchange capacity of TFCM as a function of pH and $[\text{Co}(\text{en})_3]\text{Cl}_3$ concentration.	56
10.	Simultaneous exchange of Ca^{2+} and Na^+ as a function of pH and counterion concentration ratio	58
11.	Simultaneous exchange of $[\text{Co}(\text{en})_3]^{3+}$ and Ca^{2+} from a solution 0.01 N with respect to each ion.	62

Guidance Committee:

The Paper-Format was adopted for this thesis in accordance with departmental and university regulations. The thesis body was separated into two sections. The first section was prepared for publication in Plant Physiology and has been accepted for publication. The second section is intended for publication in Planta (Berl.) and was styled accordingly.

GENERAL INTRODUCTION

The cuticle of plants is a biopolymer composed of hydroxy fatty acids linked by ester, ether and peroxide bonds and is interspersed with waxes and numerous other substances. It forms a continuous layer covering all above-ground plant parts and its differentiation must be considered as a prerequisite for terrestrial plant life. The cuticle forms the interphase between the living plant tissue and the hostile environment, characterized by its water saturation deficit, pests, diseases and, of more recent origin, pollutants.

The cuticle has been the object of many investigations and information available on its structure and chemistry is extensive. On the other hand, information about cuticle dynamics is sketchy at best in spite of the abundance of data accumulated since radio-tracers have become available. However, the interpretation of these data remained difficult and often unsatisfactory because a general theory was lacking. Progress made in surface chemistry and in the physical chemistry of polyelectrolytes within the last decades has provided essential information for better understanding the functioning of cuticular membranes.

With this background it became possible to attack and resolve some basic problems, which have been the subject of controversy for some time and which are of theoretical significance for the plant scientist as well as of practical importance to horticulturists in solving current day problems in plant protection, growth and development.

The first investigation is a quantitative study of wetting of the cuticle and the application of capillary theory to the problem of liquid entry into stomata. The second is concerned with the electrochemical properties of cuticular membranes such as exchange capacity and counterion selectivity. After establishing these basic parameters it becomes possible to apply the theory of ion exchange and transport in ionic membranes to problems such as leaching, cuticular penetration and cuticular transpiration.

SECTION I

*PENETRATION OF STOMATA BY LIQUIDS: DEPENDENCE
ON SURFACE TENSION, WETTABILITY AND
STOMATAL MORPHOLOGY*

INTRODUCTION

The penetration of liquids into the intercellular air space of leaves through open stomata has received considerable attention. There is general consensus that pure water does not enter into the intercellular space through open stomata (4, 22, 27) unless external pressure is applied (6, 7). Some organic liquids, however, are known to penetrate readily which led to attempts to estimate the degree of stomatal opening from substomatal penetration of certain organic liquids (18, 22, 25). Reports concerned with the effect of surfactants on promoting penetration into stomata and the substomatal space by aqueous solutions are contradictory (3, 4, 11, 14). Surface tension, viscosity, contact angle, diameter of the stomatal aperture, final height and initial velocity of capillary rise have been implicated in controlling penetration of liquids into the stomatal pore and substomatal chamber (4, 6, 7, 18, 26, 27); however, the relationship between any of these parameters and penetration has been generally poor. In this paper we present a systematic assessment of stomatal penetration by liquids based on the theory of capillary rise.

THEORY

When a liquid enters a capillary of circular cross-section the pressure difference (P) across the liquid meniscus is represented by Eq. 1,

$$P = \gamma_L \left(\frac{1}{R_1} + \frac{1}{R_2} \right) \quad [1]$$

where γ_L represents the surface tension of the liquid and R_1 and R_2 the principal radii of curvature of the liquid meniscus (1). In a narrow cylindrical capillary the meniscus is a segment of a sphere; R_1 and R_2 are equal and can be expressed in terms of the advancing contact angle (θ_A) and the radius of the capillary (r):

$$R = \frac{r}{\cos \theta_A} \quad [2]$$

The advancing contact angle being defined as that contact angle formed by a liquid advancing over a dry surface. Substituting Eq. 2 into 1 one obtains:

$$P = \frac{2 \gamma_L \cos \theta_A}{r} \quad [3]$$

A liquid will rise in the capillary spontaneously only if P is positive. The sign of P is determined by the term $\cos \theta_A$; P being positive when $\theta_A < 90^\circ$, zero when $\theta_A = 90^\circ$ and negative when $\theta_A > 90^\circ$. The magnitude of P increases as r decreases.

For a conical capillary (Figure 1) the angle of the capillary wall (ϕ) must be considered as an additional variable. For a converging capillary Eq. 2 becomes

$$R = \frac{r}{\sin (\phi_1 + \theta_A)} \quad (4)$$

and for a diverging capillary

$$R = \frac{r}{\sin (\phi_2 - \theta_A)} \quad (5)$$

Substituting Eq. 4 or 5 into 1, one obtains for a conical converging capillary

$$P = \frac{2 \gamma_L \sin (\phi_1 + \theta_A)}{r} \quad (6)$$

and for a diverging capillary

$$P = \frac{2 \gamma_L \sin (\phi_2 - \theta_A)}{r} \quad (7)$$

as previously derived by Adam (1).

The important difference compared to the cylindrical capillary [Eq. 3] is that the sign of P is now determined by both θ_A and ϕ . In a converging capillary P will be positive when $(\phi_1 + \theta_A) < 180^\circ$ and negative when $(\phi_1 + \theta_A) > 180^\circ$. In a diverging capillary P will be positive only when $0 < (\phi_2 - \theta_A) < 180^\circ$ or $\phi_2 > \theta_A$,

Figure 1.--Schematic drawing of a conical capillary. The wall angles (ϕ_1 and ϕ_2) in the converging and diverging portion are identical and equal to 45° . The menisci of three hypothetical liquids forming contact angles of 25° (θ_A'), 45° (θ_A'') or 90° (θ_A'''), respectively, are indicated. Note that in the converging portion ($\phi_1 + \theta_A$) is always less than 180° , the penetrating pressure therefore is positive as indicated by the positive curvature of all three menisci, and all three liquids will rise in this portion of the capillary. At the constriction the capillary diverges and only the liquid for which $\theta_A' = 25^\circ$ will rise in this portion of the capillary because $\phi_2 > \theta_A'$ and the penetrating pressure remains positive. The other two liquids will not pass the constriction as the penetrating pressure is either zero ($\phi_2 = \theta_A''$) or negative ($\phi_2 < \theta_A'''$).

Figure 2.--Schematic drawing of an Amaryllis-type stoma. The direction of penetration is indicated by the arrow.

Figure 3.--Infiltration chamber. The leaves were affixed lower surface up to the support approximately 1 cm below the cover. Thus, without applied pressure the leaf surface was subjected to a hydrostatic pressure of 1 cm of water. This value was taken into account in determining P_{ext} .

negative when $\phi_2 < \theta_A$ and zero when $\phi_2 = \theta_A$, as shown in Figure 1.

Stomata may be viewed as narrow capillaries having inclined walls. In a typical *Amaryllis*-type stoma (12, 20) (Figure 2), a zone of increasing diameter (zone 1) formed by the outer ledges is followed by a zone of decreasing diameter approaching a minimum in the pore (zone 2). Toward the substomatal chamber the radius again increases and the wall angle approaches zero at the boundary of the inner cavity and the substomatal chamber (zone 3). Therefore, Eq. 6 is applicable to zone 2 and Eq. 7 to zones 1 and 3, while Eq. 3 is not applicable. Since stomata are not generally circular cones but rather elliptic cones or elliptic paraboloids (12, 20, 26), the penetrating pressure can be approximated by substituting $\frac{2r_1r_2}{r_1+r_2}$ for r in Eqs. 6 and 7, where r_1 and r_2 represent the semiminor and semi-major axes, respectively.

Any liquid will enter and penetrate a stoma only if $P > 0$. Stomatal dimensions generally favor a finite pressure; r_1 or r_2 will never be so large as to make P infinitely small. Thus, in stomata the relationship between wall and contact angles becomes the sole determinant of the sign of P . Entry of liquids into stomata and substomatal chambers will be determined by the conditions

prevailing in those zones where the radii increase in direction of penetration, that is, in zones 1 and 3 (Figure 2). Here, capillary rise will occur only if $\theta_A < \phi_2$. In zone 2 of stomata, representing a converging capillary, P will be positive as long as $(\phi_1 + \theta_A) < 180^\circ$, a condition which will be met by most, if not all, stomata and liquids except mercury.

From these considerations the following predictions can be made and experimentally tested:

(a) Any liquid forming a zero contact angle with the wall of the stomatal aperture will enter and penetrate stomata and substomatal chambers spontaneously.

(b) Any liquid forming a contact angle less than the minimum wall angle in zones 1 and 3 will penetrate into the substomatal chamber.

(c) Any liquid forming a contact angle greater than the wall angle will not enter and not penetrate the substomatal chamber spontaneously, but can be forced to enter by application of external pressure (P_{ext}). The magnitude of P_{ext} can be calculated from Eq. 7 and depends on the contact angle and stomatal opening, such that (a) when r is constant P_{ext} will be proportional to the contact angle and (b) when the contact angle is constant P_{ext} will be inversely proportional to stomatal opening.

EXPERIMENTAL

Stomatal Frequency, Distribution
and Morphology

Frequency and distribution of stomata on leaves of Zebrina purpusii, Brückn., were determined by scanning electron microscopy.

Whole leaves with open stomata were frozen quickly on dry ice and lyophilized. Small segments (3 X 5 mm) were removed from the freeze dried leaves and mounted on a carbon slurry on carbon specimen holders. The leaf tissue was coated with carbon and gold:palladium (ca. 200 Å) before viewing with an electron microprobe X-ray analyzer (EMX-SM, Applied Research Laboratory, Inc.).

For transmission electron microscopy whole leaves with open stomata were fixed in 10% acrolein at 0 C for 24 hr. Segments (1 X 10 mm) were cut, postfixed with 2% OsO₄ in 0.1 M potassium phosphate buffer, dehydrated in a graded series of hexylene glycol and embedded in a vinyl-cyclohexane based resin according to Spurr (24). Thin sections were cut with a Porter-Blum ultramicrotome (Sorvall MT 2) using a glass knife. A Phillips EM 100 B electron microscope was employed.

Surface Tension Determinations

Solutions differing in surface tension were prepared by adding selected surfactants to deionized distilled

water having a surface tension of $72.6 \text{ dyne cm}^{-1}$. Tween 20 (polyoxyethylene sorbitan monolaurate), Triton X-100 (octyl phenoxy polyethoxy ethanol), Multi-Film X-77 (compounded product of alkyl aryl polyethoxy ethanol and free fatty acids) and Vatsol OT (dioctyl ester of sodium sulfosuccinic acid) were used. The surface tension of water, ethanol, butanol, 1,4-dioxane and aqueous surfactant solutions was determined from the maximum pull on a platinum ring suspended from the left arm of a chainomatic balance. Measured values were corrected using Harkin's and Jordan's correction tables (13). The platinum ring was cleaned by flaming between determinations and all glassware was cleaned with concentrated sulphuric acid containing 40 g/liter sodium dichromate. Since the surface tension of dilute surfactant solutions changes markedly with time, sufficient time (up to 1 hr) was permitted to establish equilibrium. Three determinations were made for each solution at 21 C. Reproducibility was 0.5 dyne cm^{-1} .

Contact Angle Measurements

Advancing contact angles of water and surfactant solutions were determined on the lower surface of leaves of Z. purpusii. The youngest fully expanded leaves free of surface contamination and defects, of greenhouse grown

plants were harvested and placed in the dark to ensure stomatal closure. Leaf strips 5 mm in width were cut perpendicular to the midrib. One leaf strip from each of five different leaves was selected for each concentration and surfactant. Five contact angle determinations were made on each strip. The strip was placed lower side up on a moist filter paper positioned on the stage of a horizontal microscope. A 2 μ l drop was formed on the tip of a microsyringe and carefully placed on the leaf. The drop was slowly built up by adding small amounts of liquid until a constant maximum contact angle was obtained. The height (h) and base width (x) of the drop were measured with a horizontal microscope fitted with an eyepiece micrometer. Measurements were made at 21 C. The contact angle was calculated using Mack's formula (16),

$$\theta_A = 2 \tan^{-1} (h/x).$$

This procedure has been shown to be very accurate for droplets which are segments of a sphere, this being the case for small droplets where the contact angle is not larger than 90° (5, 16). The largest contact angle observed in this study was 88.1°.

Since contact angles were measured immediately after the droplet had been built up, the angles reported herein are not truly equilibrium angles. However, the error was small, as contact angles on similar surfaces were found to decrease only slightly (2 to 3°) over one hr (2). The error due to surface roughness was negligible.

The roughness factor (σ), defined as $\cos \theta'_A = \sigma \cos \theta_A$ (28), where θ'_A is measured on a rough and θ_A on a smooth surface of identical composition, was estimated to be 1.01. θ'_A was measured on a positive silicon rubber replica of the leaf surface and θ_A on a smooth silicon rubber surface.

Determination of Infiltrating Pressure (P_{ext})

To obtain maximum stomatal opening consistently, leaves of Z. purpusii were placed in Plexiglas chambers at 100% relative humidity and CO₂ free air with approximately one air change per minute. Temperature was 25 C and light intensity 800 ft-c. from fluorescent (cool white) lamps. Leaves were pretreated for 30 min to effect opening, then quickly transferred into the infiltration chamber (Figure 3), attached to the leaf holder lower surface up, the chamber was sealed and pretreatment continued for 10 min. During this equilibration time the chamber was partially filled with test solution and submerged in a water bath at 25 C. Following equilibration, the chamber was filled with the test solution and pressure was applied to the solution reservoir. Near the point of infiltration the rate of increase of pressure was approximately 5000 dyne cm⁻² min⁻¹. Infiltration occurred almost instantaneously and was macroscopically apparent as infiltrated areas appeared dark in incident and bright in

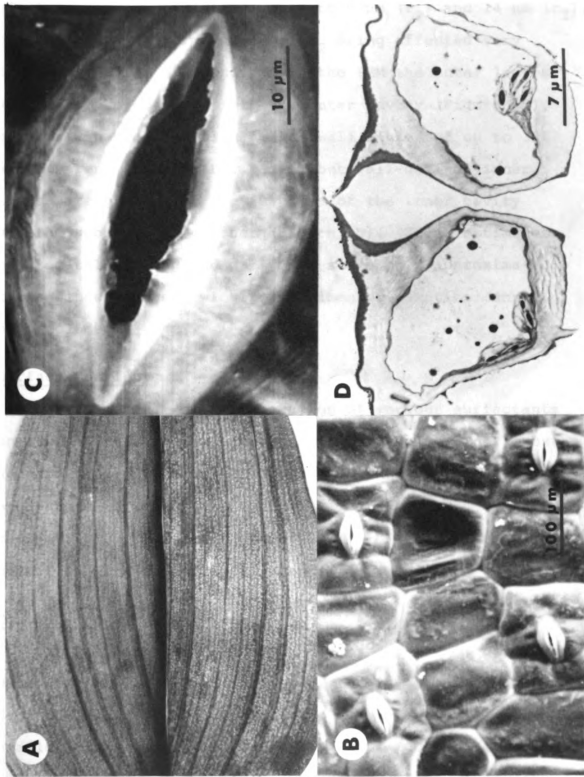
transmitted light (Figure 4A). The presence of the test solution in the substomatal chamber rather than in the stomatal aperture per se was responsible for these infiltration spots. The pressure required to effect infiltration of 10 to 20% of the stomata was recorded for each leaf and will be noted as the infiltrating pressure (P_{ext}). The pressure required to effect infiltration of only 10 to 20% of the stomata was selected to minimize a build up of pressure in the intercellular space resulting from the displacement of air by the penetrating solution. This error was considered small, as the infiltrated solution was not expelled after the pressure was released. Three determinations on four leaves each were made for each test solution. In the experiment to establish the effect of stomatal opening on P_{ext} , the pretreatment was conducted in the infiltration chamber and P_{ext} determined after prescribed time intervals. Stomatal opening was estimated following infiltration using a light microscope.

RESULTS

Frequency and Morphology of Stomata

Leaves of Z. purpusii are hypostomatous with stomata arranged in rows parallel to the veins (Figure 4B). Frequency and size of stomata varied little among leaves. There were 625 stomata per cm^2 ($s_{\bar{x}} = 0.25$). Stomatal

Figure 4.--Photomicrographs of the leaf surface and stomata of Z. purpusii. Two leaf halves photographed with transmitted light (A), upper half was not infiltrated, lower half infiltrated with surfactant solution. Infiltrated regions appearing as bright spots in the lower half-leaf. Scanning electron micrograph (SEM) of the lower leaf surface (B). SEM of an open stoma (C). Transmission electron micrograph of a cross-section of a stoma (D).



opening between the outer ledges as determined from scanning electron micrographs (SEM) was 2 to 5 μm (r_1) and 14 μm (r_2), respectively, the dimensions of r_2 being affected very little by degree of opening. In the SEM the outer ledges appear to project down into the outer cavity (Figure 4C), however, in cross-section finite wall angles of up to 30° are apparent (Figure 4D). Small but well-defined inner ledges are present at the juncture of the inner cavity and the substomatal chamber (Figure 4D). These estimates of stomatal opening and wall angles are only approximations since changes owing to specimen preparation cannot be precluded.

Surface Tension

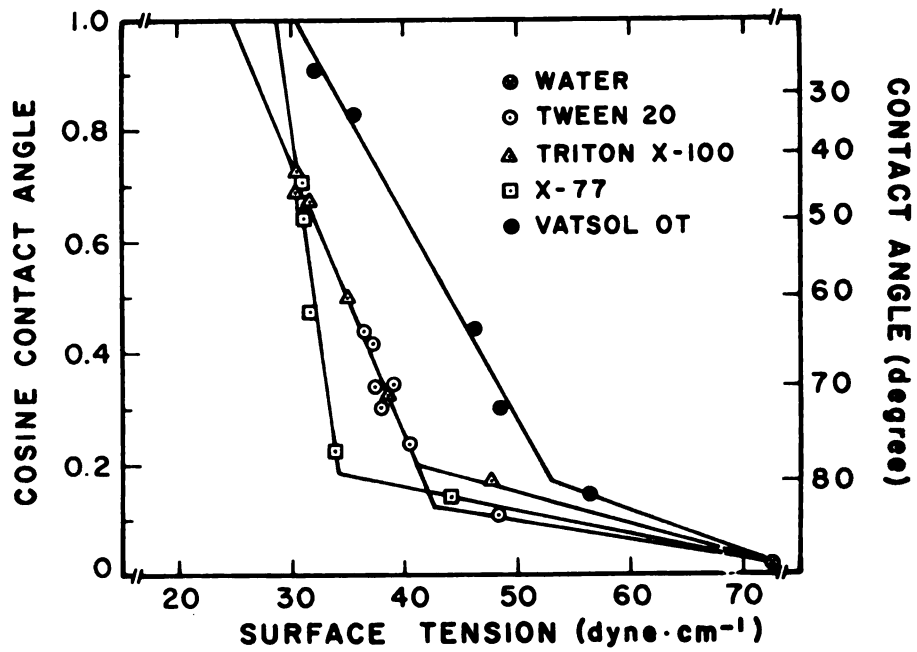
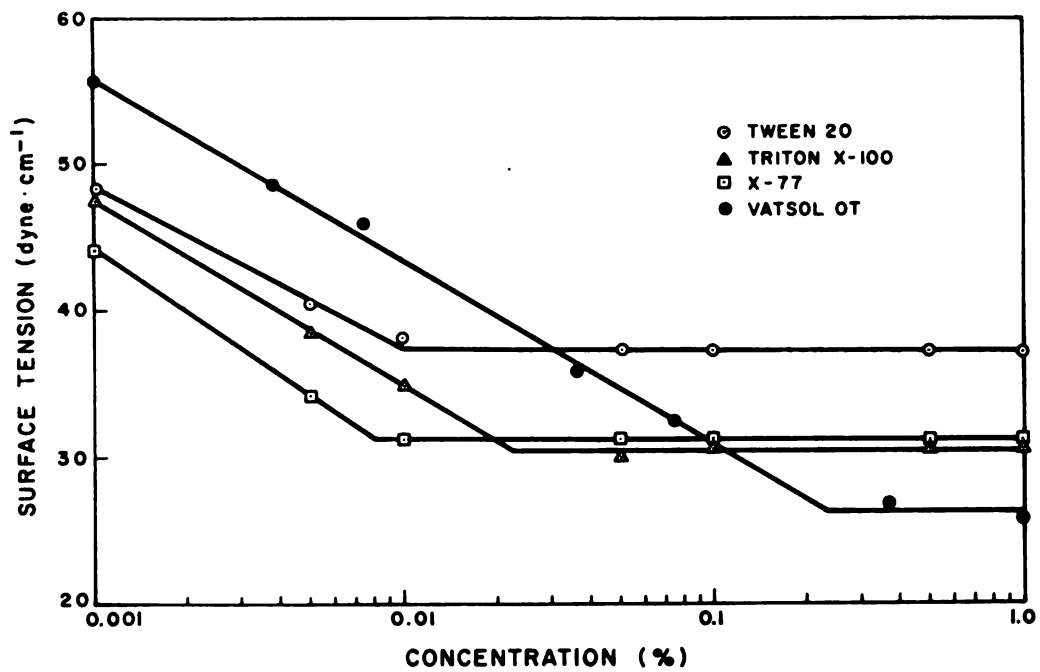
The effect of concentration of various surfactants on surface tension is illustrated in Figure 5. The lowest surface tensions obtained for Tween 20, X-77, Triton X-100 and Vatsol OT were 36.6, 30.9, 30.4 and 25.5 dyne cm^{-1} , respectively. The point of inflection of each curve coincides with the critical micelle concentration (19).

Contact Angles

The advancing contact angle of distilled, deionized water on the lower leaf surface of Zebrina was 88° . Surfactant solutions of lower surface tension produced smaller contact angles (Figure 6). Extrapolation of the curves to $\cos \theta_A = 1.0$ gives the critical surface tension

Figure 5.--The effect of surfactant concentration on surface tension of aqueous solutions.

Figure 6.--Contact angles formed on the lower surface of Z. purpusii leaves by surfactant solutions of different surface tensions (Zisman plot).



(γ_c) for the lower surface of the Zebrina leaf of 25 to 30 dyne cm^{-1} . The critical surface tension of a solid surface is defined as that liquid surface tension above which all liquids show finite contact angles (2). Thus, only liquids with a surface tension less than 30 dyne cm^{-1} will wet ($\theta_A = 0$) the lower surface of Zebrina leaves. Of the test solutions used only Vatsol OT at concentrations greater than 0.1% resulted in zero contact angle (Figure 5).

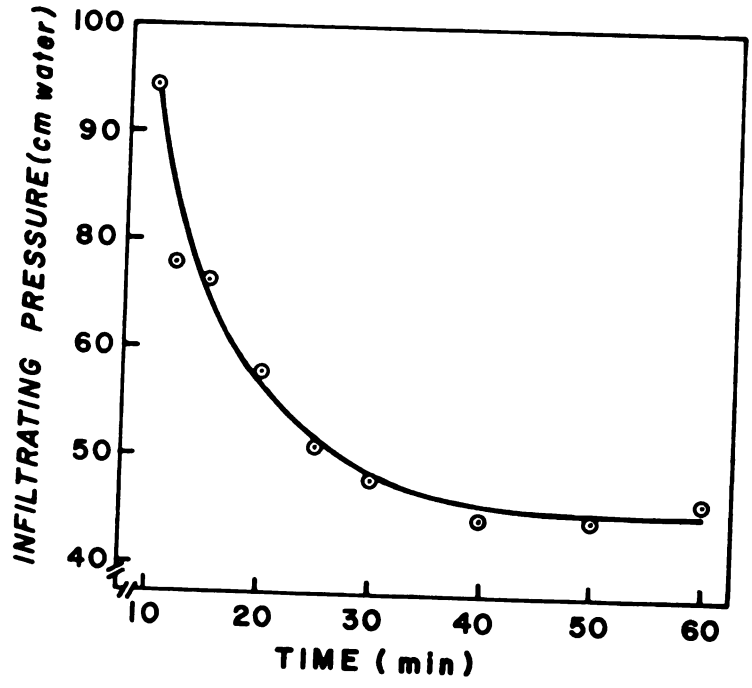
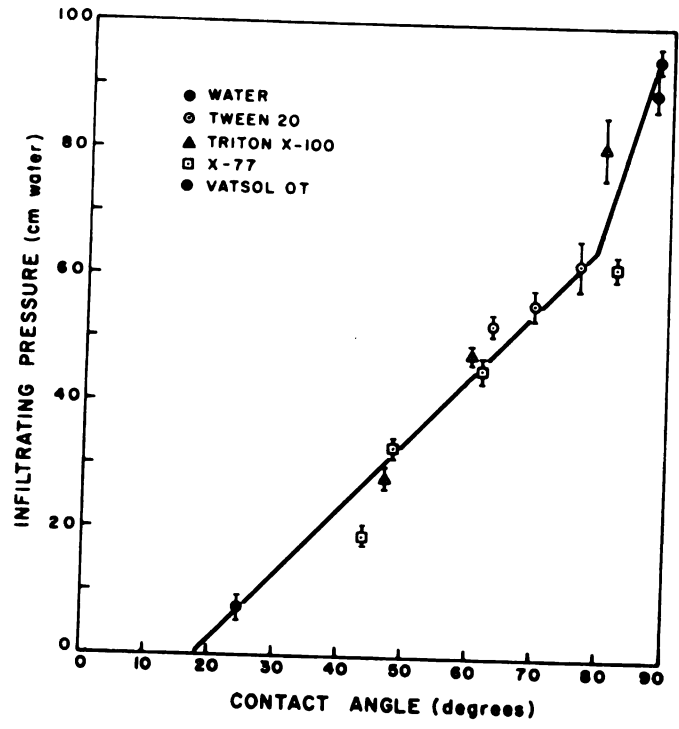
Infiltration

Solutions having $\gamma_L > 30$ dyne cm^{-1} did not penetrate through open stomata and into the substomatal chamber spontaneously. Only Vatsol OT solutions having $\gamma_L < 30$ dyne cm^{-1} infiltrated leaves spontaneously as did ethanol (21.4 dyne cm^{-1}) and butanol (23.7 dyne cm^{-1}), while 1,4-dioxane (32.4 dyne cm^{-1}) did not.

Solutions having $\gamma_L > 30$ dyne cm^{-1} could be forced into the substomatal chamber by applying external pressure. P_{ext} was directly proportional to the contact angle formed on the lower leaf surface (Figure 7). A straight line relationship was obtained in the range where the Zisman plot was linear (30 to 80°). The line fitted by inspection extrapolates to zero pressure at approximately 17°, indicating that solutions forming $\theta_A = 17^\circ$ would theoretically penetrate open stomata of Zebrina leaves.

Figure 7.--Relationship between contact angle and pressure required to infiltrate stomata of Z. purpusii.

Figure 8.--Effect of illumination period (800 ft-c) of Z. purpusii leaves on pressure required to infiltrate stomata with a Tween 20 solution forming a contact angle of 63°. Microscopic examination of the leaves established that stomatal aperture increased during the first 20 to 30 min after which no further change was observed.



These data can be interpreted to indicate a limiting wall angle in either zone 1 or 3 of 17° . However, an insufficient number of determinations at small contact angles makes this extrapolation only tentative.

The pressure required to effect infiltration of leaves with a solution forming a contact angle of 63° decreased with increasing periods of illumination, that is with increasing stomatal opening (Figure 8). A minimum value for P_{ext} was observed after 30 to 40 min when P_{ext} became time independent.

DISCUSSION

Good qualitative agreement between theoretical predictions and experimental results was obtained. Only liquids having a surface tension less than the critical surface tension as measured on the lower leaf surface of Z. purpusii penetrated into stomata and the substomatal chamber spontaneously. The critical surface tension of 25 to 30 dyne cm^{-1} observed for the surface of Zebrina leaf cuticle indicates that mainly $-\text{CH}_3-$ and $-\text{CH}_2-$ groups are exposed at the surface. The critical surface tension of pure $-\text{CH}_3$ and $-\text{CH}_2-$ surfaces has been reported to be 25 and 31 dyne cm^{-1} , respectively (23). These data are in good agreement with our current knowledge of the composition of cutin and epicuticular waxes (14). The failure of

liquids with a surface tension greater than 30 dyne cm^{-1} to penetrate stomata may be interpreted to mean that the chemical characteristics of the surface of the cuticle inside the stomatal aperture are similar to those on the leaf surface, since the critical surface tension is determined almost entirely by the nature of the chemical groups at the surface of the solid. Reports of a more polar nature of the cuticle over guard cells adjacent to the stomatal pore as indicated by staining behavior (17, 26) do not necessarily contradict our conclusion because of the limited resolution of the light microscope. From our data there would appear to be very few hydroxyl groups exposed at the surface as $-\text{CH}_2-\text{CHOH}-$ surfaces have been reported to have a critical surface tension between 35 and 42 dyne cm^{-1} (21).

The failure of liquids having surface tensions considerably larger than 30 dyne cm^{-1} to penetrate indicates that the wall angles in zones 1 and 3 must be quite small or zero. This was confirmed by microscopic observations where a very small or zero wall angle can be estimated in zone 3, largely because of the presence of the inner ledges. For zone 1 the microscopic evidence is less conclusive, for in cross-section small wall angles are evident, while SEM would indicate that the ledges are projected downward resulting in a negative wall angle. This discrepancy may be due to unknown effects of sample

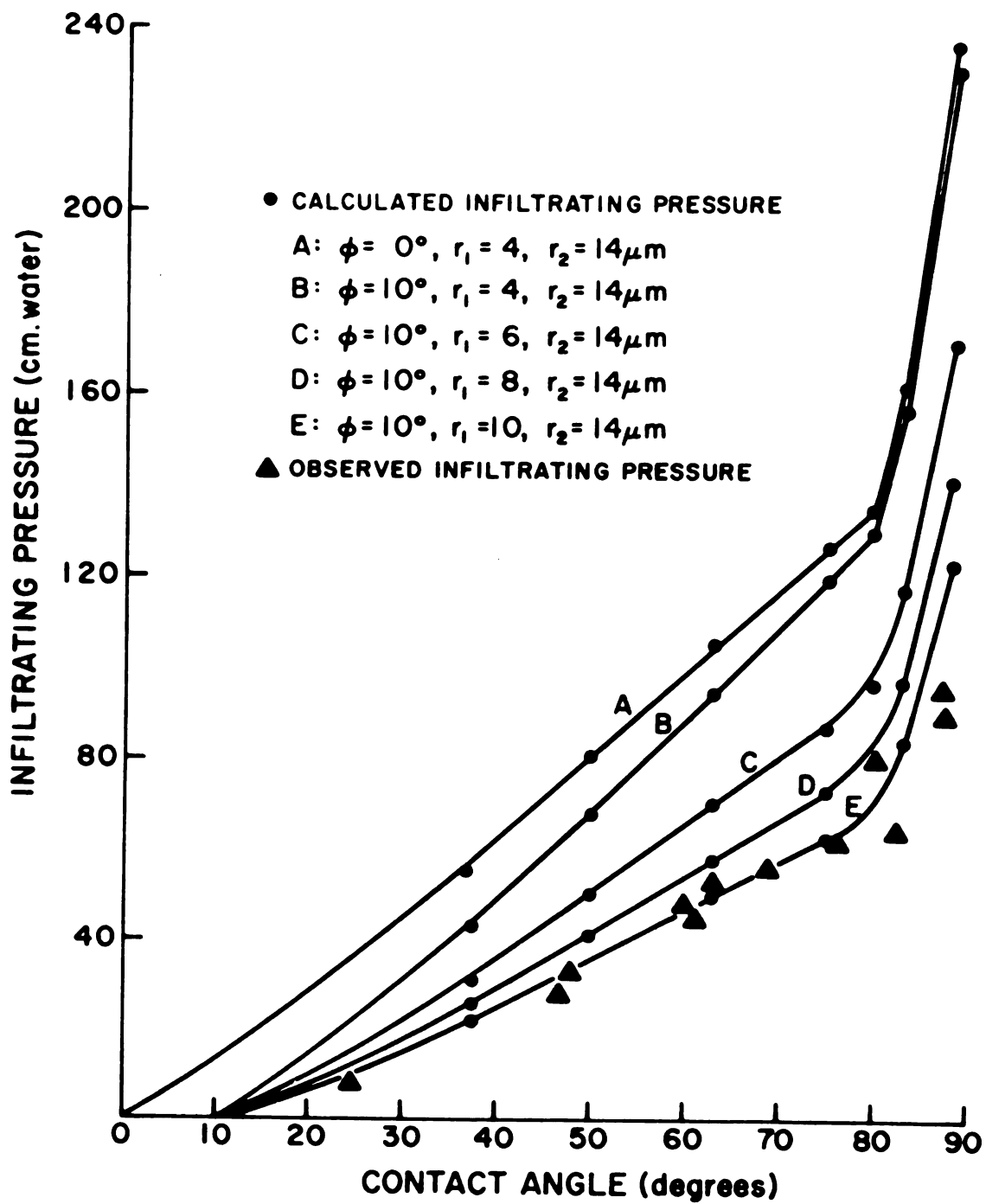
preparation. The infiltration data do not clarify this point, since they do not discriminate between entry of liquids into the stomatal aperture and into the substomatal chamber.

Liquids having a surface tension greater than 30 dyne cm^{-1} and, thus, a definite contact angle on the leaf surface could be forced into the intercellular space by application of pressure. The dependence of P_{ext} on contact angle (Figure 7) and stomatal opening (Figure 8) was as predicted; the P_{ext} was directly proportional to θ_A (at constant stomatal opening) and inversely proportional to the mean stomatal radius (at constant contact angle). A semiquantitative comparison can be made. A solution having a definite contact angle will enter a stoma up to the point where the wall angle is equal to the contact angle and where P equals zero. This is most likely to occur near the outer or inner ledges. External pressure must then be applied to force the liquid through that portion of the stomatal aperture where P is negative, that is, where the wall angle is smaller than the contact angle, and up to that point where P is again positive. Assuming limiting wall angles of zero and 10° , P_{ext} values were calculated for various values of r_1 and r_2 and plotted as a function of θ_A (Figure 9). For this purpose corresponding values for γ_L and θ_A were taken from Figure 6.

Figure 9.--Comparison of observed and calculated infiltrating pressures. Maximum infiltrating pressures were calculated from the equation

$$P = \gamma_L (r_1 + r_2) (r_1 r_2)^{-1} \sin(\phi_2 - \theta_A)$$

The value for r_2 (14 μm) was selected based on measurements of the semi-major axis (see text). The values for r_1 (4, 6, 8 and 10 μm) were selected to represent stomata of varying degrees of opening. Contact angle values corresponding to various surface tension values were taken from Figure 6.



There was a good fit between the observed P_{ext} and calculated values when r_1 equaled $10 \mu\text{m}$ and r_2 $14 \mu\text{m}$. The estimate for r_2 appears good; however, an estimate of $10 \mu\text{m}$ for r_1 appears slightly larger than that observed in the morphological studies. This is not too surprising when taking into account the approximations made in making these comparisons. The qualitative agreement between theory and experimental results was remarkably close. The data in Figure 7 demonstrate that stomatal pores cannot be assumed to be cylindrical and, therefore, earlier attempts to explain penetration of liquids on the basis of Eq. 3 were not successful (22, 26, 27).

The biological significance of the geometry of stomata and in particular the presence of outer and inner ledges must be recognized. The sudden increase in stomatal aperture with depth in zones 1 and 3 results in extremely small if not zero wall angles and, therefore, this factor becomes limiting in penetration of liquids into stomata and substomatal chambers. The low free energy surface of the cuticle resulting in large contact angles contributes to this effect. It must be stressed, however, that the large contact angle alone would not prevent infiltration of the intercellular space if stomatal apertures were cylindrical, for the contact angle of water on most leaf surfaces is smaller than 90° (5, 8, 9, 15). With stomata, the effects of small wall angles and

a low energy surface combine to present a formidable barrier to penetration of liquids with high surface tension such as water or aqueous solutions.

Our findings also provide an explanation why in earlier attempts to estimate stomatal opening from stomatal infiltration by organic liquids, only liquids with very low surface tension, such as xylene (29.0 dyne cm^{-1}), benzene (28.8), ethanol (22.3), or di(n-alkyl) ethers (25 to 28.4 dyne cm^{-1}) penetrated (18, 22, 25). A binary mixture of isobutanol and glycerol (22.6 to 44.1 dyne cm^{-1}) was used by Schorn (22) who found that stomatal penetration was rarely observed with a mixture of 29.7 dyne cm^{-1} and a mixture having 32.9 dyne cm^{-1} failed to infiltrate any of the leaves tested. This observation is in excellent agreement with ours on Zebrina leaves where the critical surface tension was 25 to 30 dyne cm^{-1} . Therefore, in these earlier infiltration experiments, most likely only liquids forming zero contact angle penetrated, which explains why the infiltration method indicated only whether or not stomata were closed, but did not indicate the degree of opening (22). This is evident from Eq. 7 showing that occurrence of non-occurrence of stomatal penetration is determined by the term $\sin(\phi_2 - \theta_A)$ and not by r (within the limits of stomatal dimensions). On the other hand, the pressure required to force a liquid into stomata having $\theta_A > \phi_2$ is related to stomatal opening Eqs. 6, 7; Figure 9) as observed by Froeschel (6, 7). Thus,

it is theoretically possible but cumbersome to determine degree of stomatal opening from P_{ext} measurements, but not by observation of spontaneous penetration by liquids having zero contact angle.

Entry of foliar sprays into stomata can also be assessed. Generally, penetration into stomata and substomatal chambers will occur when the surface tension of the spray liquid is equal or less than the critical surface tension of the leaf surface. The critical surface tension of most cuticular surfaces will be in the neighborhood of 30 dyne cm^{-1} which is the value for a $-\text{CH}_2-$ surface. Few commercially available surfactants will reduce the surface tension of aqueous solutions below 30 dyne cm^{-1} , Vatsol OT, Tergitol 7 (sodium sulfate derivative of 3,9-diethyl tridecanol-6) and Aerosol AY (diamyl ester of sodium sulfosuccinic acid) being among the most effective. There is good evidence that penetration of stomata and substomatal chambers is achieved by Vatsol OT solutions (4, 11) and these data are in agreement with our observations. Solutions forming small contact angles ($< 30^\circ$) require very little pressure to affect penetration of the substomatal chamber, a few cm of water will suffice (Figure 7). Thus, care must be exercised in interpreting data collected by submerging leaves into solutions when studying stomatal penetration (4).

LITERATURE CITED

1. ADAM, N. K. 1948. Principles of penetration of liquids into solids. *Disc. Faraday Soc.* 3: 5-11.
2. BERNETT, M. K., and W. A. ZISMAN. 1959. Relation of wettability by aqueous solutions to the surface constitution of low energy solids. *J. Phys. Chem.* 63: 1241-46.
3. CURRIER, H. B., E. R. PICKERING, and C. L. FOY. 1964. The relation of stomatal penetration to herbicidal effects using fluorescent dyes as tracers. *Weeds* 12: 301-3.
4. DYBING, C. D. and H. B. CURRIER. 1961. Foliar penetration by chemicals. *Plant Physiol.* 36: 169-74.
5. EBELING, W. 1939. The role of surface tension and contact angle in the performance of spray liquids. *Hilgardia* 12: 665-98.
6. FROESCHEL, P., and P. CHAPMAN. 1951. A new method of measuring the size of the stomatal apertures. *Cellule* 54: 233-50.
7. FROESCHEL, P. 1953. Das Druckstomatometer, ein neuer pflanzenphysiologischer Apparat zur Messung der Apertur der Stomata. *Cellule* 56: 63-70.
8. FOGG, G. E. 1948. Adhesion of water to the external surface of leaves. *Disc. Faraday Soc.* 3: 162-66.
9. FOGG, G. E. 1947. Quantitative studies on the wetting of leaves by water. *Proc. Royal Soc. B.* 134: 503-22.
10. FOY, C. L. 1964. Review of herbicide penetration through plant surfaces. *J. Agric. Food Chem.* 12: 473-77.
11. GREENE, D. W. 1969. Factors influencing the foliar penetration of naphthaleneacetic acid and naphthaleneacetamide into leaves of pear (*Pyrus communis* L.). Ph.D. Thesis, Mich. State Univ., East Lansing, Mi., U.S.A.

12. GUTTENBERG, H. V. 1959. Die physiologische Anatomie der Spaltöffnungen. In: W. Ruhland, ed., Handbuch d. Pflanzenphysiologie, Bd. XVII/1 399-414. Springer Verlag, Berlin.
13. HARKINS, W. D., and H. F. JORDAN. 1930. A method for the determination of surface and interfacial tension from the maximum pull on a ring. J. Am. Chem. Soc. 52: 1751-72.
14. HULL, H. M. 1970. Leaf structure as related to absorption of pesticides and other compounds. Residue Rev. 31: 1-155.
15. LINSKENS, H. F. 1950. Quantitative Bestimmung der Benetzbarkeit von Blattoberflächen. Planta (Berl.) 38: 591-600.
16. MACK, G. L. 1935. The determination of contact angles from measurements of the dimensions of small bubbles and drops. J. Phys. Chem. 40: 159-67.
17. MAERCKER, U. 1965. Beiträge zur Histochemie der Schliesszellen. Protoplasma 60: 173-91.
18. MOLISCH, H. 1912. Das Offen- und Geschlossenein der Spaltöffnungen veranschaulicht durch eine neue Methode (Infiltrationsmethode). Z. f. Bot. 4: 106-22.
19. OSIPOW, L. I. 1964. Surface Chemistry. Reinhold Publ. Corp., New York. pp. 163-231.
20. PISEK, A., H. KNAPP and J. DITTERSTORFER. 1970. Maximal Öffnungsweite und Bau der Stomata, mit Angaben über ihre Grösse und Zahl. Flora 159: 459-79.
21. RAY, B. R., J. R. ANDERSON, and J. J. SCHOLZ. 1958. Wetting of polymer surfaces. I. Contact angles of liquids on starch, amylose, amylopectin, cellulose and polyvinyl alcohol. J. Phys. Chem. 62: 1220-27.
22. SCHORN, M. 1929. Untersuchungen über die Verwendbarkeit der Alkoholfixierungs- und der Infiltrationsmethode zur Messung von Spaltöffnungsweiten. Jahrb. wiss. Bot. 71: 783-840.

23. SHAFRIN, E. G., and W. A. ZISMAN. 1960. Constitutive relations in the wetting of low energy surfaces and the theory of the retraction method of preparing monolayers. *J. Phys. Chem.* 64: 519-24.
24. SPURR, A. R. 1969. A low viscosity epoxy resin embedding medium for electron microscopy. *J. Ultrastructure Res.* 26: 31-43.
25. STÅLFELT, M. G. 1916. Über die Wirkungsweise der Infiltrationsmethode von Molisch und einige andere Versuche mit derselben. *Svensk. Bot. Tidskr.* 10: 37-46.
26. TURRELL, F. M. 1947. Citrus leaf stomata. Structure, composition and pore size in relation to penetration of liquids. *Bot. Gaz.* 108: 476-83.
27. URSPRUNG, A. 1925. Über das Eindringen von Wasser und anderen Flüssigkeiten in Interzellularen. *Beih. z. Bot. Zentralbl.* 41: 15-40.
28. WENZEL, R. N. 1936. Resistance of solid surfaces to wetting by water. *Ind. Eng. Chem.* 28: 988-94.

SECTION II

ION EXCHANGE PROPERTIES OF ISOLATED TOMATO

FRUIT CUTICULAR MEMBRANES: EXCHANGE

CAPACITY, NATURE OF FIXED CHARGES

AND CATION SELECTIVITY

INTRODUCTION

In recent years indirect evidence has been mounting that cuticular membranes may function as weak-acid ion exchangers. Sorption of organic ions such as dyes, 2,4-dichlorophenoxyacetic acid or naphthaleneacetic acid was found to be pH dependent; sorption of anions decreased while sorption of cations increased with increasing pH (Härtel, 1952; Orgell, 1957; Bukovac and Norris, 1966; and Morse, 1971). If sorption was plotted against pH, the curves had an inflection point between pH 2.8 and 3.2 (Bukovac and Norris, 1966). Further, surfaces of intact leaves selectively bound divalent over monovalent metal ions (Keppel, 1967). Härtel (1947, 1951) observed that cuticular transpiration was markedly dependent upon pH and nature of buffer ions used in pretreating the leaves. The order $\text{Li}^+ < \text{Na}^+ < \text{K}^+ < \text{Ca}^{2+} < \text{Sr}^{2+} < \text{Ba}^{2+} < \text{Al}^{3+}$ was observed at pH 7.0 and above, and the reverse order below pH 7. Cuticular transpiration was at a maximum at pH 7. Observations on living, detached leaves agreed with those obtained on leaves killed with chloroform vapors, pointing to a physical cause.

The fixed charge concentration of a polymer is an important characteristic affecting both sorption and transport of water and electrolytes by affecting its water content (swelling) and by imparting permselectivity to the polymer (see Lakshminarayanaiah, 1969, for an extensive discussion). Thus, the functioning of cuticular membranes will be greatly influenced by the nature and concentration of the fixed charges. The determination of these properties was the objective of this study.

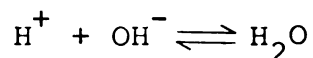
MATERIALS AND METHODS

Cuticular membranes were enzymatically isolated (Orgell, 1955; Yamada, et al., 1964) by incubating in 2% pectinase and 0.2% cellulase at pH 3.8 for about 2 weeks at 38°C. Following incubation, the cuticles were washed extensively with tap water until free of cellular debris, dried at room temperature, ground and wet sifted. The 20 to 200 mesh fraction was serially extracted (Soxhlet) with acetone, ethanol and chloroform (36 h each).

Sorbed and exchangeable electrolytes were removed by cycling the cuticular material twice between 6 N HCl and 1 N KCl, pH 11. Each acid or basic KCl wash was carried out for 12 h at room temperature and was followed by washing with deionized water until the effluent was Cl^- free. Before use, the cuticular material was converted

into the H^+ -form by a final HCl wash followed by extensive washing with deionized water to remove sorbed HCl. After these treatments tomato fruit cuticular membranes (TFCM) from ripe tomato fruits (Lycopersicum esculentum, Mill.) of the cultivar Campbell 17 had a light yellow color. This material was used in all experiments unless stated otherwise. Small quantities of cuticular material from ripe tomato fruit of the cultivar Traveller, lacking pigments in the cuticle, green pepper (Capsicum annum, L.) fruit and Brassaia (Brassaia sp.) leaves (upper astomatous cuticle only) were prepared in an identical fashion. They were opaque white in appearance.

The exchange capacity was determined by potentiometric titration. When a polymer carrying fixed acidic groups is titrated with base, e.g., NaOH, the following equilibria are established:



where R^- is the polyanion, barred quantities refer to the polymer phase. The reactions are stoichiometric which permits determination of exchange capacities from titration data provided electrolyte sorption is negligible compared to exchange. This condition was fulfilled in our study. Exchange capacity is calculated for a given pH

from the amount of base added minus the amount of base remaining at equilibrium as determined by back titration of the supernatant. In the presence of a neutral salt, e.g., NaCl, some exchange takes place even before base is added according to



and the supernatant becomes acidic. Here, the exchange was equated to the amount of H^+ released.

The progressive batch titration method was used. Portions (200 mg) of dry TFCM were weighed into 30 ml pyrex test tubes with teflon lined screw caps. Water, salt solution and standard base were added to each test tube, such that the total volume (25 ml) and salt concentration were constant and only the amount of base varied for a given experiment. Addition of water, salt solution and base was done under a stream of nitrogen or CO_2 free air, and the tubes were sealed air tight. The tubes were slowly shaken at room temperature ($25 \pm 2^\circ\text{C}$) for 4-6 d to assure equilibrium. In most cases equilibrium was achieved within 1 day, after which the pH of the supernatant no longer decreased. The TFCM was permitted to settle out before withdrawing a 10 ml aliquot of the supernatant for pH determination with a glass electrode and a Beckman Century SS pH meter, calibrated

in 0.01 pH units. A stream of CO₂-free air was bubbled through the supernatant during the pH determination until a constant reading was obtained. After reading the pH, the sample was back titrated to pH 7 with standard acid or base to determine the amount of acid released or base remaining, respectively. Each treatment was replicated twice, their pH generally agreeing within 0.05 pH units, except at inflection points where differences tended to be somewhat larger.

Solutions were prepared from reagent grade chemicals and boiled deionized water. Bases were freed from carbonate by passing through a Dowex 1-X8 column in the OH⁻-form (Davies and Nancolla, 1950) and standardized against potassium hydrogen phthalate. Tris (ethanoldiamine) cobalt(III)chloride ([Co(en)₃]Cl₃) was prepared by oxidation of an acid solution of cobaltous chloride in presence of ethylene diamine (Work, 1946). [Co(en)₃](OH)₃ was prepared by passing the chloride through a Dowex 1-X8 column in OH⁻-form. This cobalt complex is stable (Howe, 1952) and its hydroxide is water soluble.

Exchange capacities were also determined using ⁴⁵Ca labelled CaCl₂. The procedure was identical to that described above, except that the amount of Ca²⁺ left in the supernatant at equilibrium was determined by scintillation counting of 1 ml aliquots. The amount of Ca²⁺ taken

up by the TFCM was calculated from the amount of calcium added ($\text{CaCl}_2 + \text{Ca}(\text{OH})_2$) minus the amount remaining. Duplicate or triplicate determinations were made. The experimental error was less than 2%.

For brevity, methods different from these standard procedures will be given in the figure legends.

RESULTS

Effect of Pretreatment of TFCM

The titration curves obtained with $\text{Ca}(\text{OH})_2$ in the presence of 0.1 N CaCl_2 depend markedly on pretreatment (Figure 1). When pretreatment consisted of washing with deionized water only, the TFCM titrated above pH 8 with an inflection point at approximately pH 9.5. Following pretreatment with 1 N HCl a group titrating below pH 6.5 was also apparent. Repeating the 1 N HCl pretreatment had no further effect. However, if this TFCM was further treated with 1 N KCl at pH 11 and then washed with 1 N HCl the exchange capacity again increased. Repeating this procedure was again without effect. Pretreatment with stronger acid (6 N HCl) resulted in a further increase in exchange capacity. At this point, additional pretreatments with acid or basic KCl caused no further change in the titration curve. Two separate titrateable groups can be distinguished, the first between pH 3 and 6

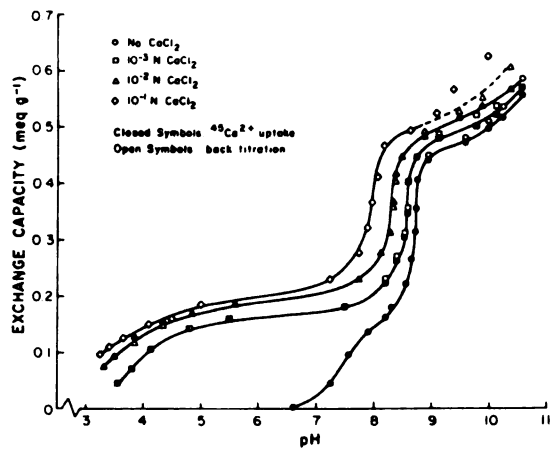
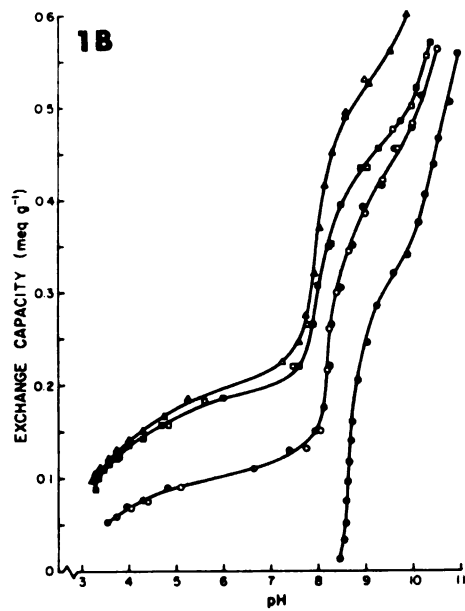
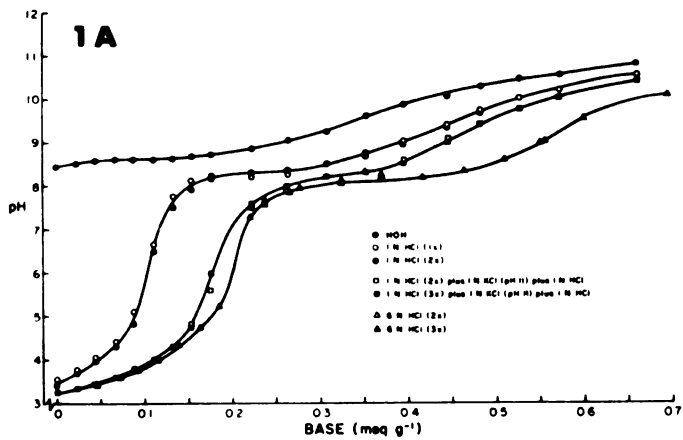
Figure 1.--Titration of TFCM with $\text{Ca}(\text{OH})_2$ in presence of 0.1 N CaCl_2 as affected by pretreatment.

A. Titration curves.

B. Exchange capacity as a function of pH.

Titration data as a function of pH corrected for H^+ released (below pH 7) or base remaining (above pH 7). The exchange capacity at any pH can be read directly from the ordinate, the first point of each curve reflects the pH depression and exchange due to CaCl_2 , without addition of base.

Figure 2.--Exchange capacity of TFCM as function of pH and CaCl_2 concentration.



(ca. 0.2 meq g⁻¹) and the second between pH 6 and 9 (ca. 0.3 meq g⁻¹). The endpoint of the third group was not reached in these experiments.

Pretreatment of TFCM with acid and alkaline KCl removed essentially all of the ash from the polymer. Total ash before pretreatment was 0.76%, while only 0.05% remained after cycling between 6 N HCl and 1 N KCl, pH 11. This last procedure was adopted as standard for all cuticular material used in the following experiments. The composition of the ash (Table 1) shows the preference of TFCM for Ca²⁺ and heavy metals which could not be completely removed. The sum of the identified cations amounts to 0.18 meq g⁻¹ TFCM, which is similar to the capacity of the first ionizable group and which was demonstrated only after cycling the TFCM (Figure 1).

Cycling TFCM between acid and basic KCl at room temperature did not appear to cause hydrolysis of polymer cross-linkages as the settled volume (swelling) of 10 ml g⁻¹ did not change. Likewise, formation of new acidic groups did not occur as the ash removed from the TFCM essentially accounted for the apparent increase in exchange capacity. However, strong alkali (1 N KOH) did cause hydrolysis and was therefore avoided.

TABLE 1.--Ash Composition of TFCM^a

	Ash Composition ($\mu\text{g g}^{-1}$)							
	Na	K	Mg	Ca	Ba	Fe	Cu	Zn
After isolation	25.5	7.8	400.0	2,431.0	208.0	69.3	120.5	35.7
After cycling ^b	0.0	0.0	0.0	0.0	0.0	3.4	33.5	0.9

^aDetermined by atomic absorption spectroscopy.

^bTFCM was cycled twice between 6 N HCl and 1 N KCl, pH 11, with intermediate and final washes with deionized water, until free of Cl^- .

Effect of Neutral Salt

The exchange capacity of the TFCM exhibited the characteristic dependence on neutral salt concentration observed with weak-acid ion exchangers. At constant pH the exchange capacity increased with increasing concentration of neutral salt (Figure 2). Here, exchange capacity was measured by two independent methods, back titration and uptake of $^{45}\text{Ca}^{2+}$ by TFCM. Excellent agreement was observed up to pH 9 above which the tracer data were consistently lower than the back titration data. Since the $^{45}\text{Ca}^{2+}$ data were obtained by measuring the decrease of the calcium concentration of the supernatant, these data represent the sum of exchangeable and sorbed calcium, because $\text{Ca}(\text{OH})_2$ and CaCl_2 may be sorbed by the TFCM in addition to exchangeable calcium associated with fixed groups. However, electrolyte sorption generally remains negligible as long as the internal (interstitial) concentration exceeds the external (solution) concentration, because of Donnan exclusion of the coion. Sorption of CaCl_2 by TFCM was negligible since ^{45}Ca data are identical to those obtained from back titration, which measures ion exchange exclusively. The discrepancy above pH 9 cannot be attributed to sorption of $\text{Ca}(\text{OH})_2$ since the ^{45}Ca data are lower than the back titration data.

Titration of Fixed Basic Groups

The difference in exchange capacity persisted up to pH 12, where both curves reach a plateau (Figure 3). This plateau denotes the total exchange capacity of TFCM as 1.05 meq g⁻¹. Subtracting the exchange capacities of the first and second groups (ca. 0.5 meq g⁻¹) leaves an exchange capacity of 0.55 meq g⁻¹ for the third group titrating between pH 9 and 12. The difference between the two curves (Figure 3) means that 0.05 meq g⁻¹ more of OH⁻ were consumed per gram of TFCM than calcium taken up. This amount of base was probably used in titrating amino groups according to



since TFCM contained 0.65% nitrogen (Table 2).

Effect of Acid Hydrolysis of TFCM

Hydrolysis of TFCM with 6 N HCl for 36 hours at 110°C resulted in loss of the first and third dissociable group (Figure 4). Upon hydrolysis TFCM also lost 13% of its original dry weight, turned brown and became difficult to wet. Contact angles greater than 90° were formed on the morphological inner surface of the membrane following acid hydrolysis, while before hydrolysis water droplets tended to spread. No nitrogen was found after hydrolysis and the oxygen content was reduced (Table 2).

Figure 3.--Exchange capacity of TFCM at high pH values as determined by back titration and $^{45}\text{Ca}^{2+}$ uptake.

Figure 4.--Exchange capacity of TFCM after acid hydrolysis as a function of pH and CaCl_2 concentration.

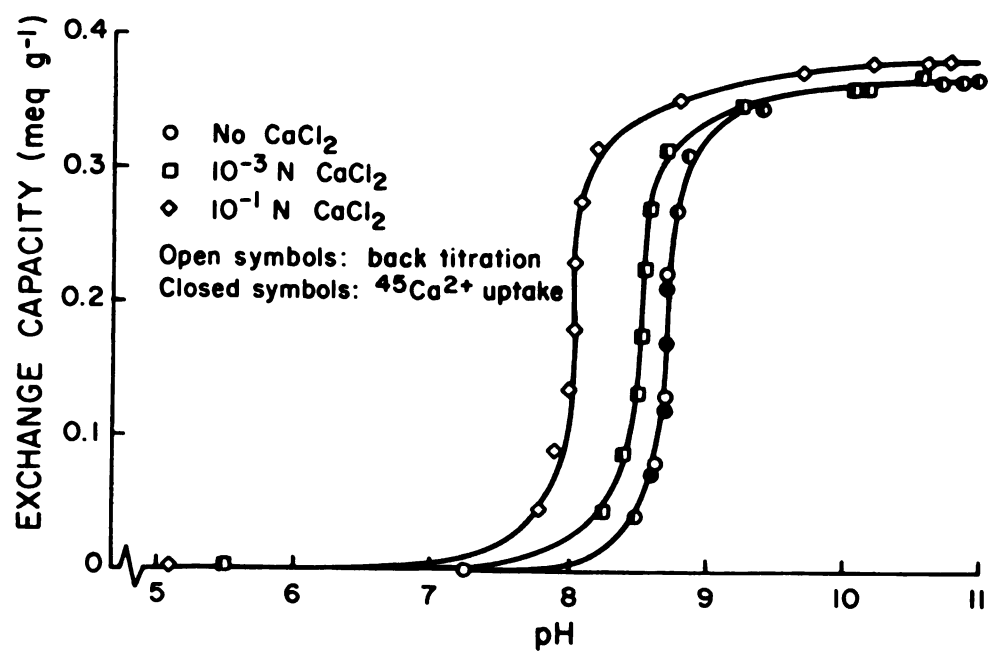
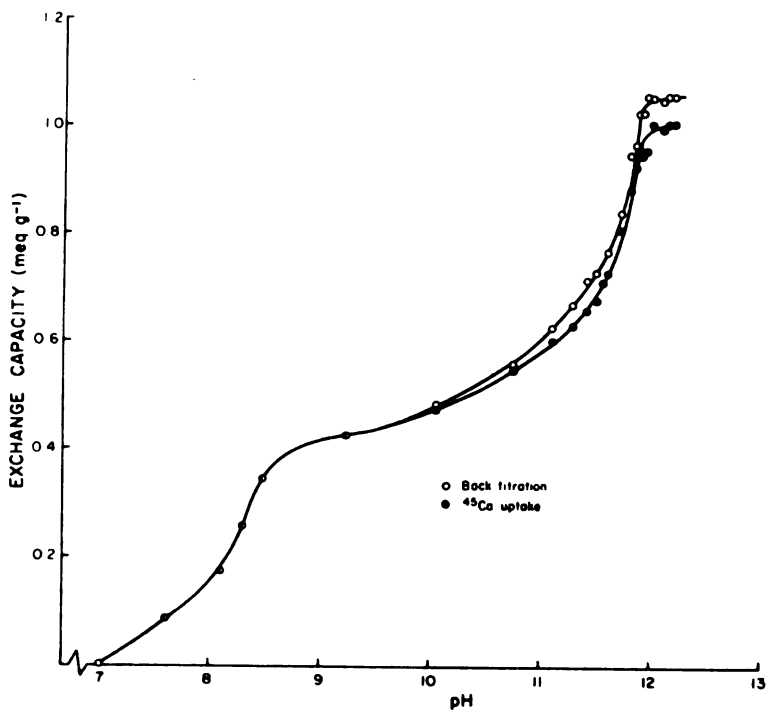


TABLE 2.--Elemental Composition of TFCM.^a

Treatment	Elemental Composition (%)				
	C	H	O	N	S
Cycled ^b (observed)	66.88	8.18	22.72	0.65	0.0
Hydrolyzed ^c (observed)	71.07	9.36	19.68	0.0	0.0
Hydrolyzed ^d (calculated)	69.7	9.7	20.7	0.0	0.0

^aAverage of duplicate determinations made by Spang, Micro-analytical Laboratories, Ann Arbor, Michigan.

^bSee legend Table 1.

^c6 N HCl for 36 hours at 110°C.

^dSee discussion.

Distinct morphological changes were also observed on the inner surface of the membrane (Figure 5) while no changes were observed on the outer surface.

The exchange capacity of the second dissociable group did not change on hydrolysis. The capacity is 0.37 meq g^{-1} ; correcting for the change in weight ($0.37 \text{ meq g}^{-1} \times 0.87$) a capacity of 0.32 meq g^{-1} was obtained, which is similar to 0.3 meq g^{-1} observed before hydrolysis. Likewise, the acid strength of the second dissociable group was not affected, as the Henderson-Hasselbalch plots (Figure 6) before and after hydrolysis coincide. Two differences, as compared to plots obtained with soluble monomeric acids, should be noted: (a) the constant n is not unity and (b) the apparent pK_a value is dependent upon the concentration of neutral salt.

*Exchange Capacities of Various
Cuticular Membranes*

Titration curves of cuticular membranes of pepper fruit, Brassia leaves and pigment free TFCM are quite similar to those presented for TFCM before (Figure 7). The titration curve for TFCM lacking pigments levels off at pH 10.

Figure 5.--Scanning electron micrographs of the morphological inner surface (cell-wall side) of TFCM before (A, B) and after (C, D) hydrolysis.

A piece of isolated TFCM was divided and one half subjected to acid hydrolysis. Both specimen were coated with carbon and a mixture of gold (20%) and palladium (80%) before viewing with a AMR 900 scanning electron microscope.

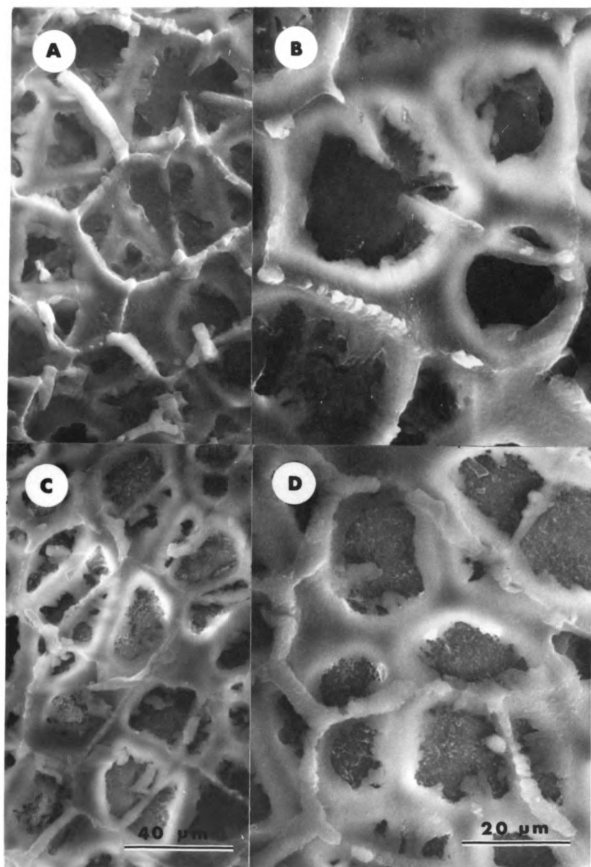


Figure 6.--Henderson-Hasselbalch plot for the second dissociable group of TFCM.

From the Henderson-Hasselbalch equation

$$\text{pH} = \text{pK}_a - n \log \frac{1 - \alpha}{\alpha}$$

where n is a constant (slope) and α is the degree of dissociation of fixed dissociable groups. $\text{pK}_a = \text{pH}$, when $\alpha = 0.5$.

Figure 7.--Exchange capacities of cuticular membranes of pepper fruit, tomato fruit cv. Traveller and Brassaia leaf as function of pH at 0.1 N CaCl_2 .

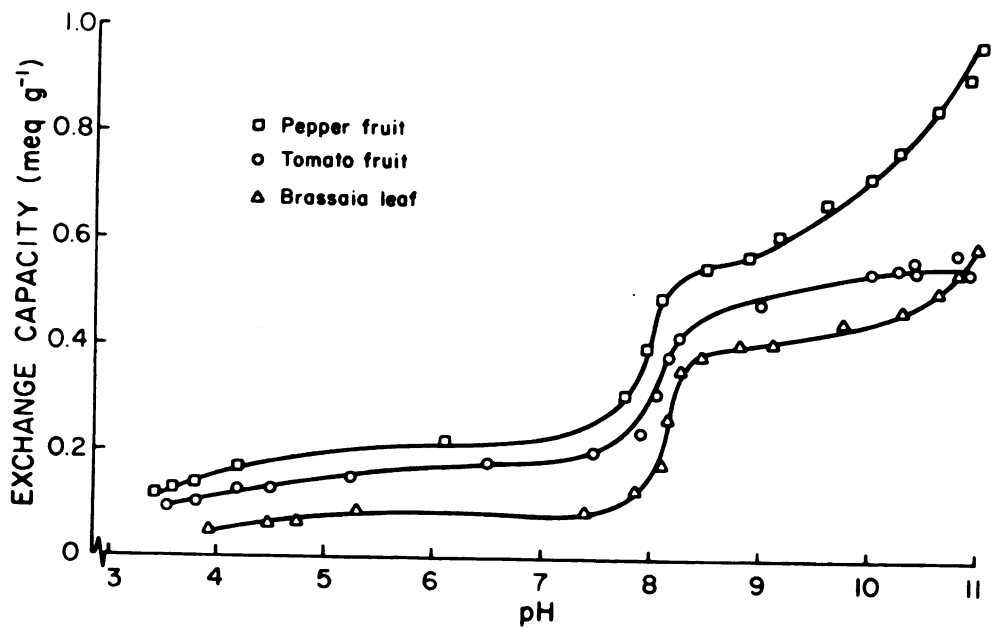
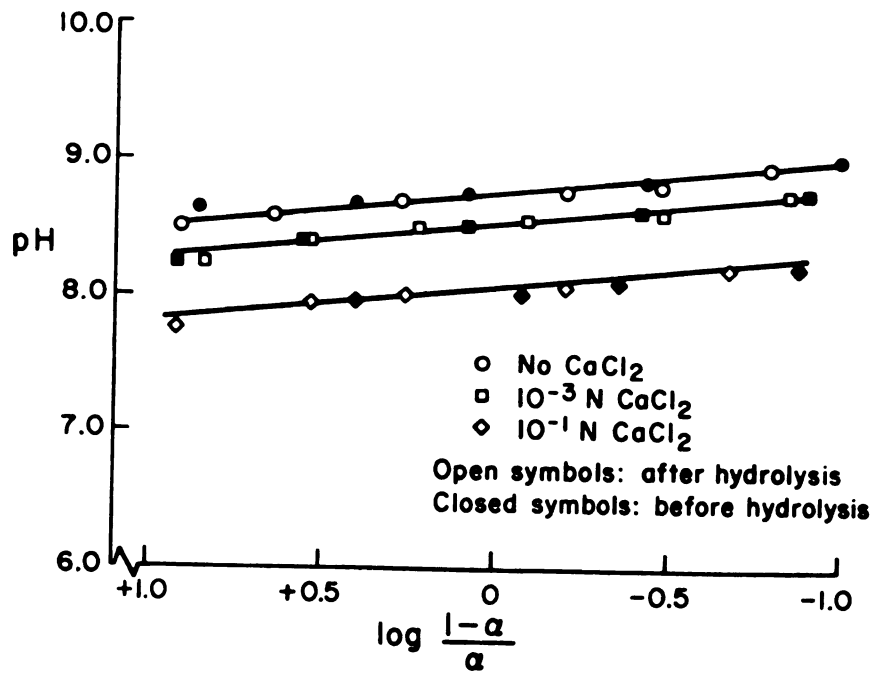


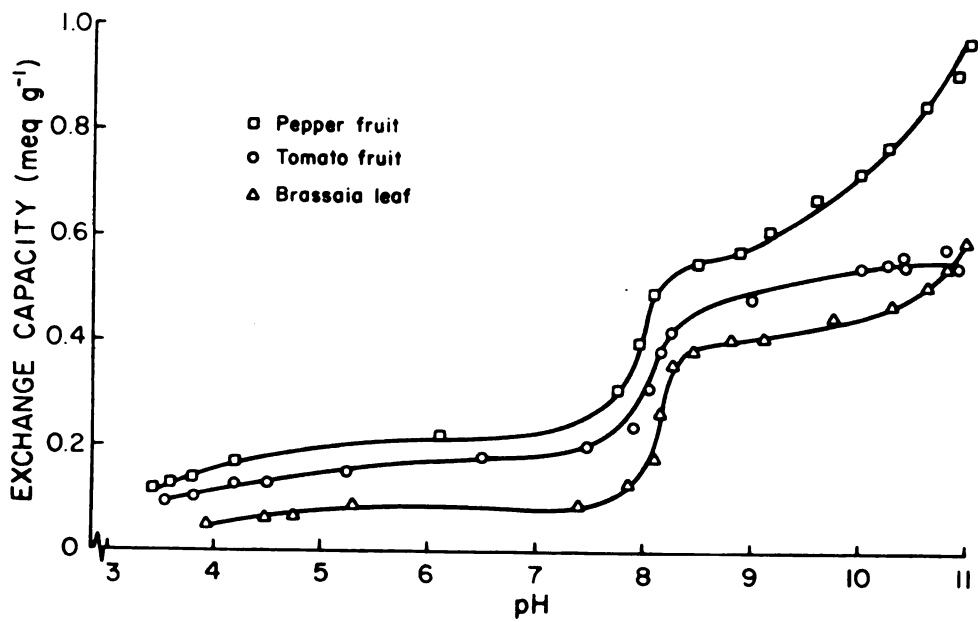
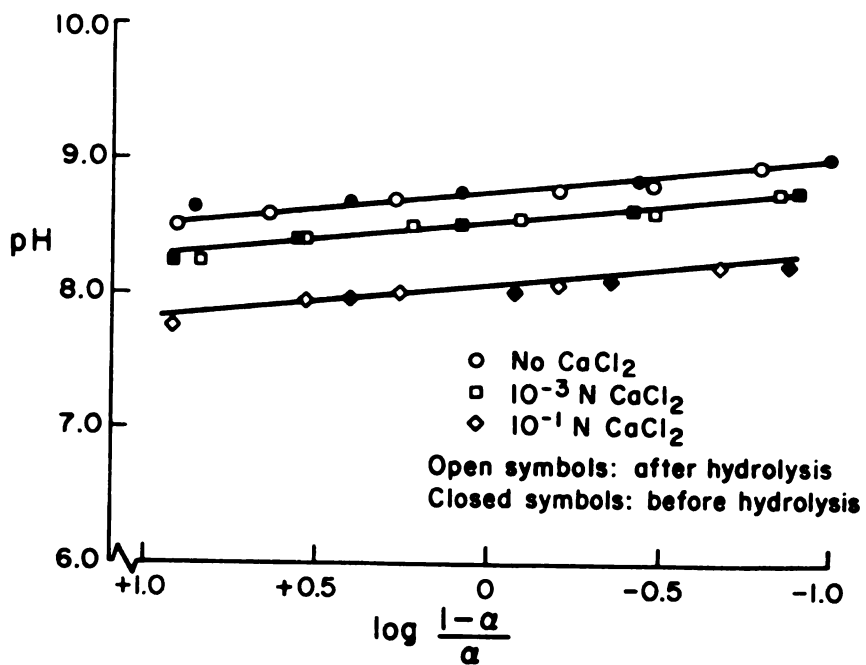
Figure 6.--Henderson-Hasselbalch plot for the second dissociable group of TFCM.

From the Henderson-Hasselbalch equation

$$\text{pH} = \text{pK}_a - n \log \frac{1 - \alpha}{\alpha}$$

where n is a constant (slope) and α is the degree of dissociation of fixed dissociable groups. $\text{pK}_a = \text{pH}$, when $\alpha = 0.5$.

Figure 7.--Exchange capacities of cuticular membranes of pepper fruit, tomato fruit cv. Traveller and Brassaia leaf as function of pH at 0.1 N CaCl_2 .



2

Effect of Nature of Counterion

The exchange capacity of TFCM was also dependent upon the nature of the counterions. At constant neutral salt concentration and pH 9 the order of decreasing capacity is $[\text{Co}(\text{en})_3]^{3+} = \text{Ca}^{2+} > \text{Ba}^{2+} > \text{Li}^+ > \text{Na}^+ > \text{Rb}^+ > \text{N}(\text{CH}_3)_4^+$ (Table 3). This order was apparent over the pH range of 3 to 10, even though small differences between ions of equal valence do not show up in the graph (Figure 8). As the affinity between fixed groups and counterions decreases the inflection points become less distinct. This is amplified with large counterions such as $\text{N}(\text{CH}_3)_4^+$ and $[\text{Co}(\text{en})_3]^{3+}$ where steric hindrance becomes a factor (Figures 8 and 9).

Counterion Selectivity

Counterion selectivity was studied by titrating TFCM in solutions of various $\text{Na}^+/\text{Ca}^{2+}$ ratios. The total exchange was determined from back titration, the Ca^{2+} exchange from $^{45}\text{Ca}^{2+}$ uptake and the Na^+ exchange was calculated from the total exchange minus the Ca^{2+} exchange. The TFCM exhibited a pronounced selectivity for Ca^{2+} ions, especially above pH 6 (Figure 10). The first and second groups behaved differently, i.e., most of the sodium is exchanged by the first group, whereas the second group exchanges measurable amounts of Na^+ only at relatively high sodium concentrations (Figure 10, B, C).

TABLE 3.--Exchange Capacity of TFCM at pH 9.0 as a Function of Nature and Concentration of Counterions.

Counterion	Exchange Capacity (meq g ⁻¹)	
	No Salt	0.1 N Salt ^a
Li ⁺	0.255	0.404
Na ⁺	0.225	0.385
Rb ⁺	0.220	0.375
N(CH ₃) ₄ ⁺	0.195	0.350
Ca ²⁺	0.450	0.515
Ba ²⁺	0.400	0.485
[Co(en) ₃] ³⁺	0.450	0.515

^aAll chlorides.

Figure 8.--Exchange capacity of TFCM as a function of
pH and nature of counterion.

Concentration of neutral salt (all
chlorides) was 0.1 N.

Figure 9.--Exchange capacity of TFCM as a function of
pH and $[\text{Co}(\text{en})_3]\text{Cl}_3$ concentration.

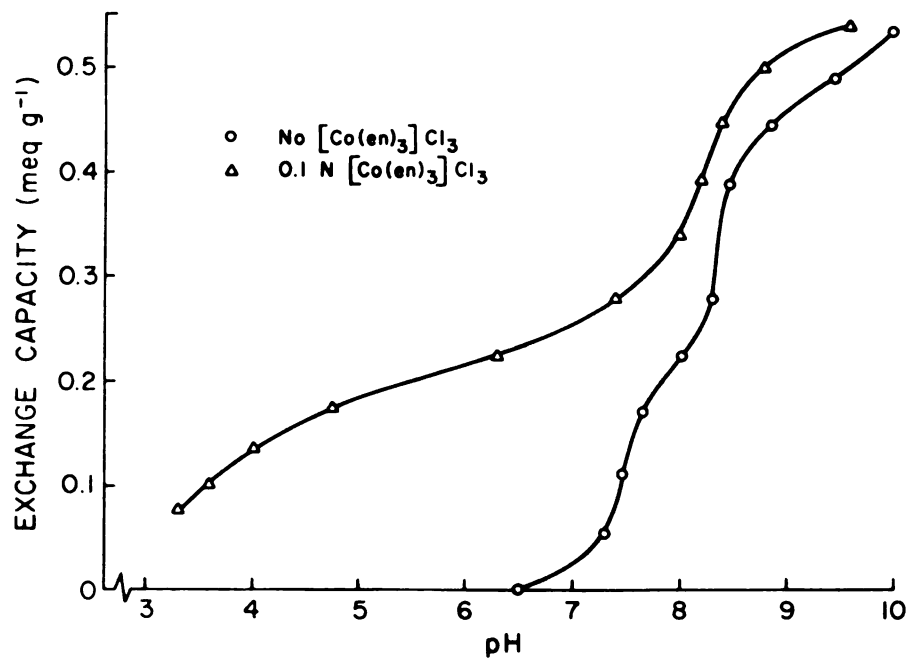
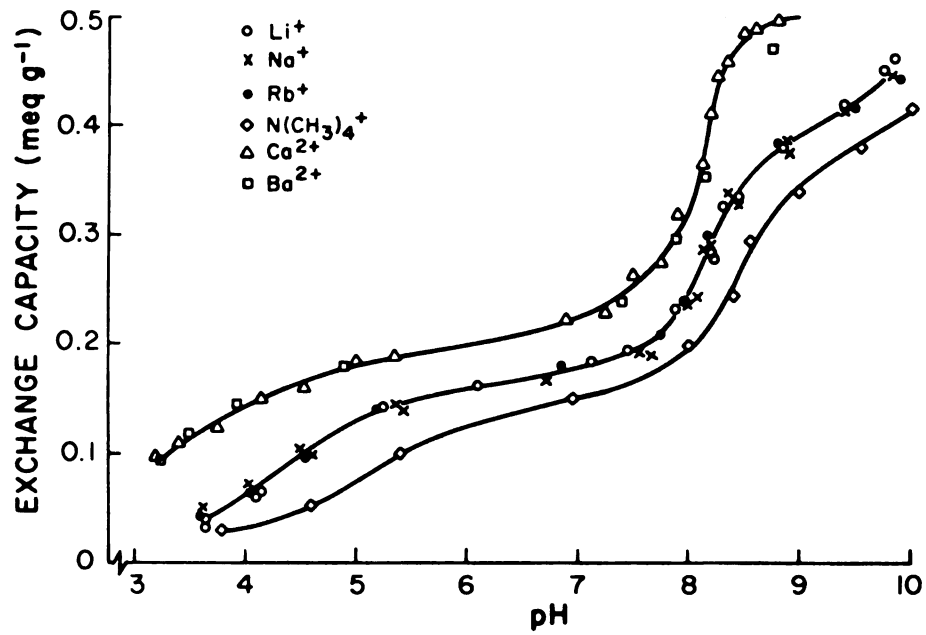


Figure 8.--Exchange capacity of TFCM as a function of pH and nature of counterion.

Concentration of neutral salt (all chlorides) was 0.1 N.

Figure 9.--Exchange capacity of TFCM as a function of pH and $[\text{Co}(\text{en})_3]\text{Cl}_3$ concentration.

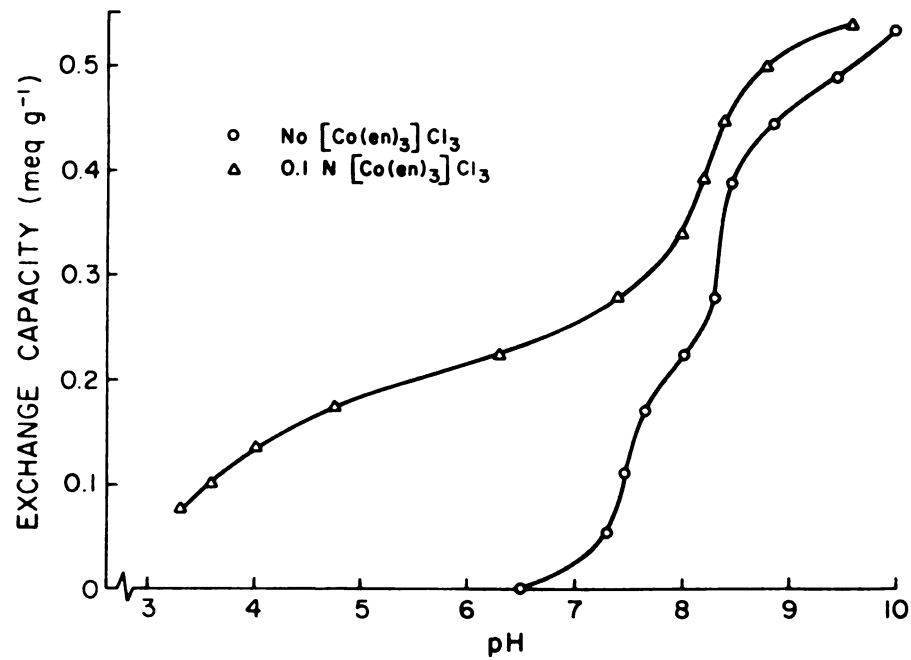
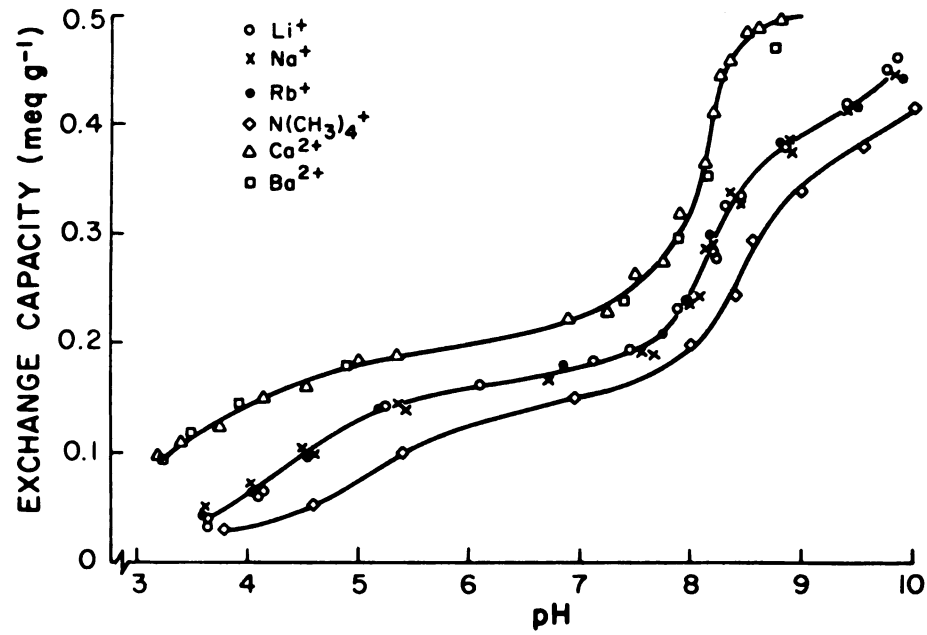
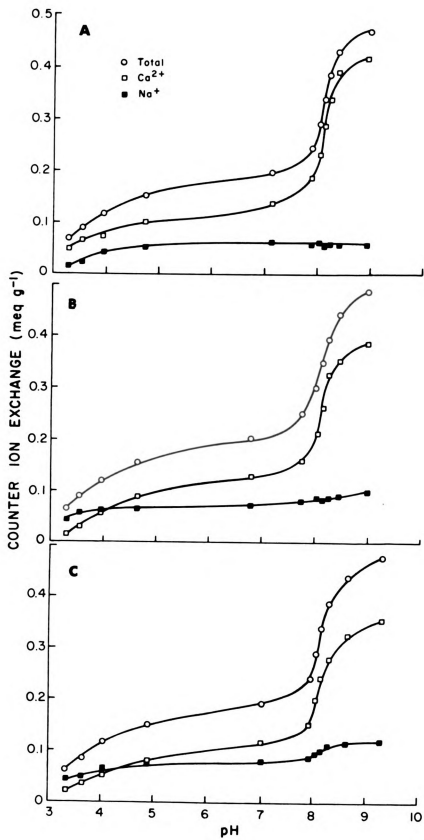
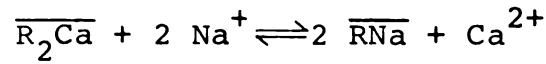


Figure 10.--Simultaneous exchange of Ca^{2+} and Na^+ as a function of pH and counterion concentration ratio.

The molal concentrations of NaCl and CaCl_2 were (A) 0.05 and 0.005; (B) 0.10 and 0.005; and (C) 0.10 and 0.0025, respectively.



Selectivity is usually expressed in terms of selectivity coefficients (K) derived from the mass action law. Since activity coefficients in the polymer phase are not known, molalities (m) are generally used and all deviations from ideality are therefore contained in the selectivity coefficients which are no longer constants, but depend on experimental conditions. The selectivity coefficient for the equilibrium



is thus defined by

$$K_{Na}^{Ca} = \frac{\overline{m}_{Ca}}{(\overline{m}_{Na})^2} \frac{(m_{Na})^2}{m_{Ca}} \quad [1]$$

The ion exchanger prefers calcium over sodium if $K_{Na}^{Ca} > 1$ and sodium over calcium if $K_{Na}^{Ca} < 1$. Since in this study the water content of the TFCM is not known, the exchangeable electrolyte in the polymer was referred to unit polymer rather than unit sorbed solvent. Thus the quantities \overline{m}_{Na} and \overline{m}_{Ca} in equation [1] were replaced by (\overline{Na}) and (\overline{Ca}) , where the latter carry the dimension millimoles g^{-1} TFCM. Selectivity coefficients so calculated are marked with an asterisk ($*K_{Na}^{Ca}$). When 1 g TFCM contains 1 g sorbed water K_{Na}^{Ca} and $*K_{Na}^{Ca}$ are numerically equal. In other cases $*K_{Na}^{Ca}$ can be converted into K_{Na}^{Ca} values by multiplying the former by the

water content of the polymer. Selectivity coefficients for the simultaneous exchange of Ca^{2+} and $[\text{Co}(\text{en})_3]^{3+}$ were derived in a similar fashion.

The observed $*K_{\text{Na}}^{\text{Ca}}$ values are large, especially at high degree of neutralization (Table 4). At $m_{\text{Na}}/m_{\text{Ca}}$ ratios of 10 and 20 selectivity coefficients decrease initially. The endpoint of the first dissociable group coincides approximately with $\alpha = 0.4$

A different picture emerges for the simultaneous exchange of Ca^{2+} and $[\text{Co}(\text{en})_3]^{3+}$ from a solution 0.01 N with respect to each ion. The trivalent $[\text{Co}(\text{en})_3]^{3+}$ was exchanged only in slightly larger quantities than Ca^{2+} (Figure 11 A) and the selectivity coefficient decreased rapidly as the equivalent ionic fraction of $[\text{Co}(\text{en})_3]^{3+}$ in the polymer increased (Figure 11 B).

DISCUSSION

Identity of Fixed Charges and Polymer Structure

Titration of TFCM with base results in titration curves indicative of three distinctly different dissociable groups, whose acid strength depends on the concentration of neutral salt and nature of counterions. This is characteristic of polymers that carry fixed weak-acid groups such as $-\text{COOH}$ or phenolic hydroxyls (Hale and

TABLE 4.--Selectivity Coefficients for the Simultaneous Exchange of Calcium and Sodium by TFCM.

m_{NaCl}	0.05	0.10	0.10
m_{CaCl_2}	0.005	0.005	0.0025
$\frac{m_{\text{NaCl}}}{m_{\text{CaCl}_2}}$	10	20	40
α^a	Selectivity Coefficients ($*K_{\text{Na}}^{\text{Ca}}$)		
0.13	53.5	10.0	21.7
0.17	34.8	9.7	33.5
0.23	10.1	16.6	26.7
0.35	10.0	27.7	32.5
0.40	11.0	27.0	43.0
0.50	16.5	29.0	51.2
0.60	24.0	35.5	60.0
0.70	35.0	42.5	69.0
0.80	47.5	49.5	75.5
0.90	55.5	57.9	87.0

^aThe fraction of fixed charges ionized (α) was calculated as $\alpha = \text{capacity}/0.50 \text{ meq g}^{-1}$.

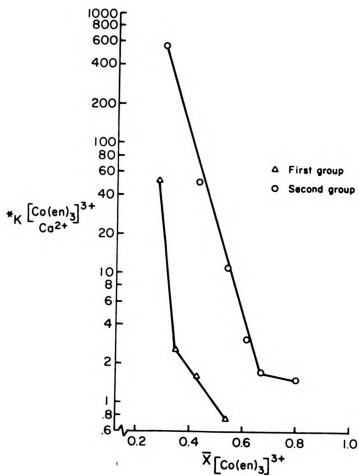
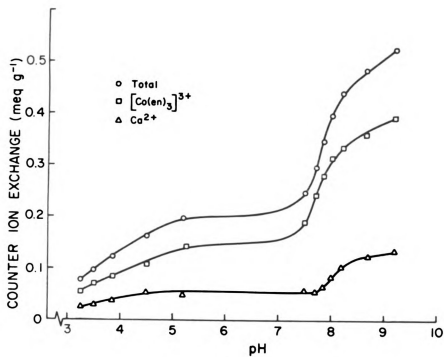
Figure 11.--Simultaneous exchange of $[\text{Co}(\text{en})_3]^{3+}$ and Ca^{2+} from a solution 0.01 N with respect to each ion.

- A. Exchange as a function of pH.
- B. Selectivity coefficients plotted as a function of the equivalent ionic fraction of $[\text{Co}(\text{en})_3]^{3+}$ in the TFCM.

Selectivity coefficients were calculated from the equation

$$*K_{\text{Ca}}^{\text{Co}(\text{en})_3} = \frac{([\text{Co}(\text{en})_3]^{3+})^2}{(\text{Ca}^{2+})^3} \cdot \frac{(m_{\text{Ca}^{2+}})^3}{(m_{[\text{Co}(\text{en})_3]^{3+}})^2}$$

Selectivity coefficients for the second group were calculated after subtracting the amounts of Ca^{2+} and $[\text{Co}(\text{en})_3]^{3+}$ bound by the first group at pH 6 from the total amount of these counterions above pH 6.



Reichenberg, 1949; Topp and Pepper, 1949; Howe, 1952; Katchalsky, 1954; Gregor, et al., 1955; 1958; and Michaeli and Katchalsky, 1957). Since sulfur was not present in the TFCM, the dissociable groups are most likely carboxyls (first and second) and phenolic hydroxyls (third), respectively. The pH range of their titration is consistent with this assignment.

Disregarding the salt and ion effect on acid strength for the moment, the maximum capacity observed was 1.05 meq g^{-1} (Figure 3) of which 0.2 meq g^{-1} can be attributed to the first and 0.3 meq g^{-1} to the second group, respectively (Figure 2). Based on acid strength of the groups, the composition of TFCM (Brieskorn and Reinartz, 1967) and cuticular membranes in general (Mazliak, 1968; Martin and Juniper, 1970) and by reference to titration curves of polymers of known composition (Speiser, et al., 1945; Topp and Pepper, 1949; Deuel, et al., 1953a, 6; Gregor, et al., 1955; Howe and Kitchener, 1955; Hutschneker and Deuel, 1956; Michaeli and Katchalsky, 1957), the first group can tentatively be assigned to pectic substances, the second to non-esterified hydroxy fatty acids and the third to phenolic hydroxyls.

The picture is somewhat complicated by the presence of nitrogen in the TFCM. It is unlikely that



this nitrogen is a contaminant of the enzymes used for isolation in view of the rigorous washing and cycling before using the TFCM for titration. Proteins (0.5%N) have earlier been reported in apple fruit cuticular membranes (Huelin, 1959) and enzymes have been implicated in cutin synthesis (Heinen and Brand, 1963). Cell-wall enzymes also may be occluded during cutinization of epidermal cell walls which is quite extensive in tomato (Figure 5).

The 0.65% figure for nitrogen means that roughly 4 g protein was contained in 100 g TFCM. The contribution of acidic (aspartic and glutamic acid) and basic (lysine) groups can be approximated, since the composition and number of charges of globular proteins do not vary greatly (White, et al., 1964). Using β -lactoglobulin for example, we have 13 g lysine per 100 g protein (Leggett-Bailey, 1967), that is approximately 0.036 meq lysine g^{-1} TFCM. Similarly, there are 1.4 meq titratable $-\text{COOH}$ groups g^{-1} protein (Timasheff, 1970), that is 0.057 meq g^{-1} TFCM. These groups titrate between pH 4.1 to 4.5 (aspartic and glutamic acid) and pH 9.6 to 10.4 (lysine) (Timasheff, 1970, p. 5). The discrepancy between the titration curve and ^{45}Ca -binding above pH 9 (Figures 2 and 3) may thus be attributed to titration of lysine amino groups. The agreement between observed (0.05 meq g^{-1}) and calculated (0.036 meq g^{-1}) capacity is fair

considering the crudeness of the approximations. The contribution of aspartic and glutamic acid residues to the first group amounts to approximately 28%.

The first and third dissociable groups were not present after acid hydrolysis, while the second was not affected (Figure 4). Thus, 0.73 meq g^{-1} ($1.05-0.32$) were lost together with 130 mg g^{-1} TFCM of weight, including all of the nitrogen. The weights, calculated from the known capacities of the components and their equivalent weights (Table 5) add up to 127 mg which is in excellent agreement with the 130 mg figure observed. Confirmation can be made also by subtracting the calculated sums of the weights of C, H, O and N of the components (Table 5) from the composition of the polymer before hydrolysis (Table 2) and calculating the theoretical composition of TFCM after hydrolysis. Again, the observed and calculated values agree quite well (Table 2) which lends support to the partitioning shown in Table 5.

The contribution of flavonoids to the exchange capacity of the third group is also demonstrated by the color change of TFCM from yellow to deep red on titration above pH 10, and the absence of the third titrateable group in the tomato variety Traveller lacking pigments in the cuticle (Figure 7).

TABLE 5.--Estimated Contribution of Proteins, Pectic Substances and
and Flavonoids to the Exchange Capacity of TFCM.

Component	Exchange Capacity meq g ⁻¹	Equivalent Weight g meq ⁻¹	Total Weight mg g ⁻¹	Weight of Elements mg g ⁻¹			
				C	H	O	N
Protein (-COOH) (-NH ₃ ⁺)	0.057 0.050	•	40	21.0	2.8	8.6	6.5
Pectic Substances	0.143	212 ^a	30	10.2	1.7	18.1	0
Naringenin ^b	0.237	90	22	14.5	1.0	6.5	0
Quercitrin ^b	0.237	149	35	19.4	1.6	13.5	0
SUM	0.724		127	65.1	7.1	46.9	6.5

^aEquivalent weight of galacturonic acid.

^bNaringenin and quercitrin were assumed to be present in equal amounts
as shown for other tomato varieties (Ming-an Wu and Burrell, 1958).

The equivalent weight of the linear sub-unit of the cutin polymer of TFCM can be calculated. Since only monocarboxylic hydroxy fatty acids were found after depolymerization of cutin (Brieskown and Reinartz, 1967), only linear polymers can be expected. These linear polymers have an average molecular weight of 2,670 ($1g/3.75 \cdot 10^{-4} \text{ eq g}^{-1}$). The molecular weights of hydroxy fatty acids found after cutin hydrolysis vary between 280 and 320, hence every ninth or tenth hydroxy fatty acid in the polymer remained non-esterified. Linear polyesters of this size are readily soluble in chloroform (Carothers and van Natta, 1933). TFCM is not chloroform soluble because of cross-linking of linear sub-units by ether and peroxide bridges (Mazliak, 1968; Martin and Juniper, 1970). Similar molecular weight estimates of 2,600 and 3,330 were obtained for the linear polyesters of cutin isolated from pepper fruit and Brassia leaves, respectively.

Effect of Neutral Salt and Nature of Counterion on Apparent Acid Strength

The apparent acid strength of dissociable groups increased with increasing concentration of neutral salt, increasing valence and decreasing crystal radius of counterions (Table 3, Figure 8). This behavior is typical for polyelectrolytes of the weak-acid type (Gregor, et al., 1955; Howe and Kitchener, 1955) and is

generally not observed with monomeric organic acids. The main reason for this behavior of polyelectrolytes is the electrostatic free energy arising from the mutual repulsion of neighboring fixed charges. As titration proceeds, an increasing number of fixed charges dissociate and neighboring fixed charges of the same sign repel each other, thus raising the electrostatic potential along the polymer chains (Katchalsky, 1954; Gregor, et al., 1955; Michaeli and Katchalsky, 1957). This repulsion causes the previously coiled polymer chains to uncoil and stretch, which concomitantly lowers the configurational entropy and increases the free energy of the polymer network. As the electrostatic potential increases during titration, the tendency to form more negative groups will diminish and the apparent acid strength therefore decreases as the degree of ionization and capacity increase.

The electrostatic free energy can be reduced by association between fixed charges and counterions and by screening of neighboring fixed charges (Howe, 1952; Katchalsky, 1954; Gregor, et al., 1955; Michaeli and Katchalsky, 1957). The smaller the crystal radius of a counterion the greater the interaction with the fixed charge, the lower the electrostatic free energy and the greater the apparent acid strength. The order of crystal

radii of counterions used in this study is $(\text{H}^+) < \text{Li}^+ < \text{Na}^+ < \text{Rb}^+ < \text{N}(\text{CH}_3)_4^+$, $\text{Ca}^{2+} < \text{Ba}^{2+} < [\text{Co}(\text{en})_3]^{3+}$, which is the order of decreasing acid strength observed (Table 3, Figures 8 and 9). With large counterions such as $\text{N}(\text{CH}_3)_4^+$ and $[\text{Co}(\text{en})_3]^{3+}$ steric hindrance becomes important as well, especially in polymers with a high degree of cross-linking. The tendency to form weak bonds between the hydrocarbon skeleton of these organic counterions and the polymer, which tends to increase the selectivity of the polymer to organic ions, may be counteracted or even offset by steric hindrance hampering the approach between counterion and fixed charge. The effect of $\text{N}(\text{CH}_3)_4^+$ on decreasing the acid strength of TFCM is an illustration of this effect and is an indication of the presence of rather narrow intermolecular spaces (pores) (Figure 8).

Increasing the concentration of neutral salt increases the apparent acid strength because (a) the sorbed electrolyte tends to shield neighboring fixed charges and thus decreases electrostatic free energy, and (b) reduces the Donnan potential, that is, reduces the pH difference between external solution and polymer (Michaeli and Katchalsky, 1957). Since in these experiments sorption was very small, the Donnan potential and thus the pH difference must have been large. The following considerations illustrate the magnitude of the combined

effects of the electrostatic free energy and the Donnan potential. The intrinsic pK_a of hydroxy fatty acids is approximately 5 (Albert and Serjeant, 1962). The apparent pK_a observed with TFCM for the second group are 8.75, 8.50, and 8.00 at zero, 0.01 and 0.1 N $CaCl_2$, respectively (Figure 6). Hence, the apparent pK_a of the $-COOH$ groups were 3.0 to 3.75 pH units higher than the intrinsic pK_a of this group.

Counterion Selectivity

TFCM showed a pronounced selectivity for Ca^{2+} over Na^+ . From a solution having a Na^+ concentration 40 times that of Ca^{2+} the polymer exchanged up to 2.8 times more Ca^{2+} than Na^+ (Figure 10 C). The cause is similar to that discussed previously. If two ions are available, the polymer preferentially exchanges that ion which results in the minimum free energy, that is, the polymer prefers the counterion that associates more closely with the fixed charges (minimizing the electrostatic free energy) and which results in the smallest polymer volume (minimizing the free energy of stretching and maximizing the configurational entropy of the polymer chains (Gregor, et al., 1958). In comparison with sodium, the divalent calcium ion associates more closely with the fixed charges and reduces swelling because only one half the number of osmotically active particles are present. Exchangeable



calcium ions also tend to have a lower osmotic coefficient than sodium (Howe, 1952).

Interpretation of selectivity coefficients

($*K_{Na}^{Ca}$) is difficult without knowing the water content of the TFCM. Preliminary experiments gave an estimate of 100 to 200 mg water g^{-1} TFCM. The degree of ionization or nature of counterion had little effect. Thus, as a first approximation, TFCM prefers Ca^{2+} over Na^{+} if $*K_{Na}^{Ca} > 5$ to 10. Selectivity coefficients increased with increasing degree of ionization (Table 4). The second dissociable group ($\alpha = 0.4$ to 1) showed a greater selectivity than the first. Since above $\alpha = 0.4$ selectivity coefficients are averages of the first and second dissociable group, the true values for the second group will be larger than shown. The initial decrease of selectivity coefficients at low ionic strength may be explained by the observation that the selectivity of cross-linked polygalacturonic acid decrease with increasing capacity (Deuel, et al., 1953), an anomaly still unexplained. This was not evident at higher ionic strength, possibly because selectivity tends to decrease with increasing ionic strength.

The trivalent $[Co(en)_3]^{3+}$ is initially strongly preferred over Ca^{2+} (Figure 11), but the selectivity is reversed as the equivalent ionic fraction of $[Co(en)_3]^{3+}$

in the polymer is increased. Sterically $[\text{Co}(\text{en})_3]^{3+}$ is very large compared with Ca^{2+} ; while initially preferred because it results in lower osmotic pressure and because of weak bonds between the ethanoldiamine ligands and the TFCM, these factors are offset later because of the volume effect on the polymer. Another possible explanation for the selectivity reversal is that a fraction of the fixed charges is located in narrow pores not readily accessible to $[\text{Co}(\text{en})_3]^{3+}$.

It should be stressed that selectivity is difficult to explain without data on water content and polymer volume (swelling). In absence of such information the above explanations must be considered tentative having been based on the behavior of polymers of known composition, swelling and water content. The fact remains, however, that TFCM shows a pronounced selectivity typical of ion exchangers with a high degree of cross-linking and high fixed charge density, whose water content is small because of limited swelling.

The selectivity of TFCM is remarkable in view of its relatively low exchange capacity. At low degrees of neutralization the average charge density is low. Assuming a specific gravity of TFCM of 1.1 g cm^{-3} and a uniform distribution of fixed charges, the distance between fixed charges would be 24.6, 8.4 and 6.7 \AA at capacities of 0.10, 0.25 and 0.50 meq g^{-1} , respectively.

These distances are too great to give rise to large electrostatic potentials, which could account for the selectivities observed, at least at low degrees of ionization. Most likely the fixed charges are not uniformly distributed, but probably clustered. Likewise, a random distribution of -COOH groups in TFCM, consisting of mainly long CH_2^- skeletons, would be unfavorable energetically and therefore not very probable. If this is the case, then the important question is the distribution of the clusters within the membrane and whether or not they are oriented in such a way to form the polar channels often hypothesized (see e. g. Hull, 1970). Localized preferential permeability to Hg^{2+} (Schönherr and Bukovac, 1970) and a nonhomogeneous distribution, in cross-section, of electron dense heavy metal stains in cuticular membranes (Maier, 1968), have been demonstrated.

Before the biological significance of these findings can be assessed information concerning the water content and charge distribution are required. The nature of buffer ions and the pH have been shown to affect cuticular transpiration (Härtel, 1947, 1951). These observations were explained by assuming that cuticular transpiration was controlled by an ampholyte (the cuticle?) having very narrow pores and an isoelectric point around pH 7. Ions with large hydration shells were thought to reduce cuticular transpiration by reducing the amount of

free water in the pores (water not part of hydration shells). From our work with TFCM and Brassia leaf cuticular membranes, it appears that cuticular membranes carry mostly acidic groups and a reversal of the net charge from positive to negative at pH 7 is thus not very likely. It should also be remembered that counterions in weak-acid type ion exchangers have very small hydration shells, if any (Gregor et al., 1955, 1958; Howe and Kitchener, 1955).

A final note of caution. The above data were obtained using TFCM from which all extractable materials had been removed. They amount to approximately 5% of the initial dry weight (Morse, 1971) and the total exchange capacity of TFCM is expected to be somewhat higher due to extractable fatty acids and selectivity of non-extracted TFCM may also differ somewhat due to effects of embedded waxes on the elasticity of the polymer. It is possible that structural changes in the TFCM may have taken place during isolation and extraction but in the absence of any definite evidence to this effect it is assumed that, with the exception of the effects due to removal of extractable materials, the properties of TFCM used in this study are those exhibited by TFCM in its natural state.

REFERENCES

- Albert, A., Serjeant, E. P.: Ionization constants of acids and bases, p. 124. New York, John Wiley and Sons Inc., 1962.
- Brieskorn, C. H., Reinartz, H.: Zur Zusammensetzung der Tomatenschale. II. Alkalilösliche Anteile. Zeitschr. Lebensmittel-Untersuchung und Forschung 135: 55-58 (1967).
- Bukovac, M. J., Norris, R. F.: Foliar penetration of plant growth substances with special reference to binding by cuticular surface of pear leaves. In: VI Simposio Internazionale de Agrochimica sul 'Transporto delle molecole organiche nelle piante.' pp. 298-309. Varenna, 5-10 Settembre, 1966.
- Carothers, W. H., Natta, F. J. van: Studies of polymerization and ring formation. XVIII. Polyesters from ω -hydroxydecanoic acid. J. Am. Chem. Soc. 55: 4714-4719 (1933).
- Davies, C. W., Nancolla, G. H.: Preparation of carbonate-free sodium hydroxide. Nature (Lond.) 165: 237-238.
- Deuel, H. K., Hutschneker, K., Solms, J.: Selektives Verhalten von Ionenaustauschern. Z. f. Elektrochem. 57: 172-178 (1953a).
- _____, Solms, J., Altermatt, H.: Die Pektinstoffe und ihre Eigenschaften. Vierteljahresschr. Naturforsch. Ges. Zürich 98: 49-86 (1963b).
- Gregor, H. P., Hamilton, M. J., Becher, J., Bernstein, F.: Studies on ion exchange resins XIV. Titration, capacity and swelling of methacrylic acid resins. J. Phys. Chem. 59: 874-881 (1955).
- _____, Hamilton, M. J., Oza, R. J., Bernstein, F.: Studies on ion exchange resins. XV. Selectivity coefficients of methacrylic acid resins toward alkali metal cations. J. Phys. Chem. 60: 263-267 (1958).

- Hale, D. K., Reichenberg, D.: Equilibrium and rate studies of cation exchange with monofunctional resins. *Disc. Faraday Soc.* 7: 79-90 (1949).
- Härtel, O.: Über die pflanzliche Kutikulartranspiration und ihre Beziehungen zur Membranquellbarkeit. *Sitzungsber. Akad. Wiss. Wien, math. nat. Kl. Abt. I* 156: 57-86 (1947).
- _____ : Ionenwirkung auf die Kutikulartranspiration von Blättern. *Protoplasma* 40: 107-136 (1951).
- _____ : Färbungsstudien an der pflanzlichen Kutikula. *Protoplasma* 41: 1-14 (1952).
- Heinen, W., Brand, I. V. D.: Enzymatische Aspekte zur Biosynthese des Blattcutins bei *Gasteria verrucosa* Blättern nach Verletzung. *Z. Naturforschung* 18 b: 67-79 (1963).
- Howe, P. G.: Studies in ion exchange. Ph.D. thesis, University of London, London, England, 1952.
- _____, Kitchner, J. A.: Fundamental properties of cross-linked polymethacrylic acid ion exchange resins. *J. Chem. Soc.* 1955: 2143-2151 (1955).
- Huelin, F. E.: Studies on the natural coatings of apples. IV. The nature of cutin. *Austral. J. Biol. Sci.* 12: 175-180 (1959).
- Hull, H. M.: Leaf structure as related to absorption of pesticides and other compounds. *Residue Rev.* 31: 1-155 (1970).
- Hutschneker, K., Deuel, H.: Ionengleichgewichte an Kationaustauschern verschiedener Austauschkapazität. *Helv. Chim. Acta* 39: 1038-1045 (1956).
- Katchalsky, A.: Problems in the physical chemistry of polyelectrolytes. *J. Polymer Sci.* 22: 159-184 (1954).
- Keppel, H.: Cation exchange phenomena in plant leaves. In: *Isotopes in Plant Nutrition and Physiology. Proceedings of the symposium on the use of isotopes in plant nutrition and physiology*, pp. 329-345, Vienna 1967.

- Lakshminarayanaiah, N.: Transport phenomena in membranes. New York, London, Academic Press, 1969.
- Leggett-Bailey, J.: Techniques in protein chemistry, p. 11. Amsterdam, London, New York, Elsevier Publ. Co. 1967.
- Maier, U.: Dendritenartige Strukturen in der Cuticularschicht von *Lilium candidum*. *Protoplasma* 65: 243-246 (1968).
- Martin, J. T., Juniper, B. E.: The cuticle of plants. Edward Arnolds (Publ.) 1970.
- Mazliak, P.: Chemistry of plant cuticles. In: Progress in Phytochem. Vol. 1, pp. 49-111. Reinhold, L., Liwschitz, Y., eds. New York, London, Interscience Publ. (1968).
- Michaeli, I., Katchalsky, A.: Potentiometric titration of polyelectrolyte gels. *J. Polymer Sci.* 23: 683-696 (1957).
- Ming-an Wu, Burrell, R. C.: Flavonoid pigments of the tomato (*Lycopersicum esculentum* Mill.). *Arch. Biochem Biophys.* 74: 114-118 (1958).
- Morse, R. D.: Sorption of methylene blue and 2,4 dichlorophenoxyacetic acid by isolated tomato fruit cuticular membranes. Ph.D. thesis, Michigan State University, East Lansing, Mich. USA. 1971.
- Orgell, W. H.: The isolation of plant cuticle with pectic enzymes. *Plant Physiol.* 30: 78-80 (1955).
- _____ : Sorptive properties of plant cuticle. *Proc. Iowa Acad. Sci.* 64: 189-198 (1957).
- Schönherr, J., Bukovac, M. J.: Preferential polar pathways in the cuticle and their relationship to ectodesmata. *Planta (Berl.)* 92: 189-201 (1970).
- Timasheff, S. N.: Polyelectrolyte properties of globular proteins. In: *Biological Polyelectrolytes*, p. 33, A. Veis ed., New York, Marcel Dekker Inc., 1970.
- _____ : p. 5.
- Speiser, R., Hills, C. H., Eddy, C. R.: The acid behavior of pectinic acids. *J. Phys. Chem.* 49: 328-343 (1945).

- Topp, N. E., Pepper, K. W.: Properties of ion exchange resins in relation to their structure. I. Titration curves. J. Chem. Soc. 1949: 3299-3303 (1949).
- White, A., Handler, P., Smith, E. L.: Principles of Biochemistry, p. 123, New York, McGraw Hill, 1964.
- Wolk, J. B.: Tris-ethylenediamine cobalt (III) chloride synthesis: In: Inorganic Synthesis, Vol. II, pp. 221-222. Fernelius, W. C., ed. New York, London, McGraw-Hill, Inc., 1946.
- Yamada, Y., Wittwer, S. H., Bukovac, M. J.: Penetration of ions through isolated cuticles. Plant Physiol. 39: 28-32 (1964).





MICHIGAN STATE UNIV. LIBRARIES



31293104453356